



ADDIS ABABA UNIVERSITY
ADDIS ABABA INSTITUTE OF TECHNOLOGY
SCHOOL OF MECHANICAL AND INDUSTRIAL
ENGINEERING

Developing pantograph-catenary contact and predicting fatigue failure of contact wire of railways

A Thesis Submitted to the Graduate School of Addis Ababa University in Partial Fulfillment of the Requirements for the Degree of Masters of Science

In Railway Engineering

(Rolling Stock)

By

Andinet Zereabruk

Advisors

Dr. Daneil Tilahun (Phd)

Mr. Habtamu Tekubet (Msc)

August 2014

ADDIS ABABA UNIVERSITY
ADDIS ABEBA INSTITUTE OF TECHNOLOGY
SCHOOL OF MECHANICAL AND INDUSTRIAL
ENGINEERING

Developing pantograph-catenary contact and predicting fatigue failure of contact wire of railways

By

Andinet Zereabruk

August, 2014

Approved by Board of Examining:

Birhanu Besheh (Dr.)

Railway Center Head

Signature

Date

Daniel Tilahun (Dr.)

Advisor

Signature

Date

Habtamu Tekubet (Mr.)

Advisor

Signature

Date

Mr. Tolosa Deribe (Msc)

Internal Evaluator

Signature

Date

Mr. Tsegaye Feleke (Msc)

External Evaluator

Signature

Date

ACKNOWLEDGEMENT

I would like to express my sincere thanks to my Advisors, Dr.Daneil Tilahun and Mr.Habtamu Tekubet, who provided me the invaluable guidance, generous support and encouragement to complete this thesis and made the research journey interesting and enjoyable. I would also like to thank my family members, closely related colleagues and friends whose minds were with me to tolerate for the work presented here.

ABSTRACT

Railway overhead systems (catenary–pantograph) are subjected to cyclic load (fatigue) while delivering electrical energy to train’s electrical motors. The catenary–pantograph system mainly consists of a messenger wire, contact wire and a pantograph. Contact between the pantograph’s head and contact wire is vital for the train to operate smoothly. Too much or too little contact leads to increased wear in the system. This cyclic load leads to fatigue wear of over head contact wire and then unexpectedly without any indication the system will fail. Hence, this thesis paper addresses the problem by developing the contact between the pantograph-catenary and then predicts the fatigue life of the contact wire. This ensures the reliability of the railway system, control their maintenance periods and the quality of the current collection will increase as the loss of contact is maintained. The methods used in this thesis are analytical system and predicting the fatigue life via ANSYS soft ware and comparing the results with experimental results carried out. The application area is in electrical driven railways via pantograph-catenary system like Ethiopian Rail way Corporation which uses light rail way in Addis Ababa city and Ethio-djibouti rail way. Thus, as results show in this thesis, it is possible to maximize the life span of the contact wire by applying preventive and proactive maintenance, minimize maintenance cost, down time of trains and increase the satisfaction of customers.

Table of Contents

ACKNOWLEDGEMENT	I
ABSTRACT	Error! Bookmark not defined.
LIST OF TABLES	V
LIST OF FIGURE.....	VI
NOMENCLATURES	VIII
CHAPTER ONE	1
INTRODUCTION	1
1.1. Back ground of research.....	1
1.2. Different catenary systems	2
1.3. Statement of the problem	3
1.4. Significance of the research	4
1.5.1. General objective of the research	4
1.5.2. Specific objective of the research	4
1.6. General methodologies.....	4
1.7. General conditions	5
1.8. General parameters	5
CHAPTER TWO	6
LITERATURE REVIEW	6
2.1. Introduction	6
2.2. Requirements of a pantograph-overhead wire while sliding contact.....	14
ANALYSIS OF PANTOGRAPH CATENARY INTERACTION.....	16
3.1. Material selection of catenary wire.....	16
3.2. Determining the contact force using European standards.....	21
3.3. Calculating the natural frequency of the system	23
3.7.1. Analysis.....	34
3.8. Displacement of the contact wire in the Y direction.....	36
3.9. Modeling the catenary wire by using ANSYS soft ware	37
CHAPTER FOUR.....	40
SIMULATION RESULTS AND DISCUSSION.....	40

4.1.	Predicting Fatigue life of the catenary wire via ANSYS soft ware	40
4.1.2.	Fatigue Sensitivity	44
4.1.3.	Hysteresis	45
4.1.4.	Damage	47
4.1.5.	Fatigue Factor of Safety at a Design Life	47
CHAPTER FIVE		53
CONCLUSION, RECOMMENDATION AND FUTURE WORK.....		53
5.1.	CONCLUSION.....	53
5.2.	RECOMMENDATION	55
5.3.	FUTURE WORK.....	56
REFERENCE		57
APPENDIX		61

LIST OF TABLES

Table 1 : Material composition of contact wire	14
Table 2 : Material property of LN2 catenary wire [12]	16
Table 3 : Material property of C270 catenary Wire [12]	17
Table 4 : Material property of Re330 catenary [12]	17
Table 5 : Materials and structure of the catenary [13]	17
Table 6 : Relating Speed of the train and driving frequency of contact wire.....	21
Table 7 : The contact force for different speed of trains	23
Table 8 : Coefficients for bodies in contact[2]	30
Table 9 : Technical specifications for relating acceleration vs speed.....	36
Table 10 : Fatigue sensitivity of contact wire by ANSYS soft ware	45
Table 11 : Stress-strain graph of contact wire via ANSYS soft ware.....	46

LIST OF FIGURE

Figure 1: Contact wire surface defects due to, electrical arcs, Corrosion and cyclic load [1].	1
Figure 2: Pantograph-catenary system [2].	2
Figure 3: Different catenary structures (a), stitched catenary (b) (often referred to as Y-line) and (c) compound catenary [2].	3
Figure 4: Bending stress vs fatigue life of contact wire	7
Figure 5: RTRI test bench for over head contact wire study [1]	12
Figure 6: Fatigue fracture obtained on the RTRI's bench [9].	13
Figure 7: Model of Pantograph-Catenary [17]	19
Figure 8: Model of catenary system as beam element [10].	19
Figure 9: Two elastic solids in contact,(a)contact configuration; (b) before loading; c) after loading xy axis coincides with major and minor axis of elliptical contact area (hatched area), (d) Displacement of the contacting point M1 and M2 and rigid distance of approach $d=d_1+d_2$ [16]	28
Figure 10: Modeling of contact wire-pantograph	31
Figure 11: Modeling of pantograph-catenary wire while sliding	33
Figure 12: Pantograph-catenary interaction	35
Figure 13: The photo shows the tensioning system of contact wire [12].	37
Figure 14: Front view of contact wire and its standard dimension.	37
Figure 15: Contact wire modeled via ANSYS soft ware	37
Figure 16: Junction claw photos [9].	38
Figure 17: Dropper clamped onto the contact wire (Photo: Petter RøeNåvik). [8]	38
Figure 18: Modeling of contact wire with junction claw via ANSYS soft ware.	38

Figure 19: a) Meshing of catenary system (left) b) Force analysis of catenary system (right)	39
Figure 20: Fatigue life of the catenary system far from the droppers.....	41
Figure 21: Fatigue life of the catenary system near o the droppers	42
Figure 22: Equivalent stress pantograph-catenary system away from the dropper.	43
Figure 23: Stress vs cycle to failure of contact wire fatigue test analysis by ANSYS soft ware.....	44
Figure 24: Fatigue damage of contact wire via ANSYS soft ware.....	47
Figure 25: Safety factor of pantograph-catenary system	48
Figure 26: Static Vonmises stress of contact wire far from the droppers	49
Figure 27: Dynamic Vonmises stress of contact wire near to the droppers	49
Figure 28: Total deformation of the contact wire in areas of droppers and far from droppers	50
Figure 29: Dynamic Vonmises stress of contact wire with and without droppers	50
Figure 30: The maximum shear elastic strain of pantograph-catenary system	51
Figure 31: Mean stress correction.....	63

NOMENCLATURES

ρ	Mass per unit length
T	Tension
w	weight per unit length
T_e	The Eigen period (cycle)
ω_e	The fundamental Eigen frequency
h_r	Hour
E	Young's modulus
EI	Bending stiffness
V	Velocity
V_{ref}	The reference speed
y_o	Vertical displacement
t	Time
m	Mass
δ_{Max}	Standard deviation
C	Damping
k	Stiffness
I	Area moment of inertia
ϵ	Strain
s	Span length

p'_o	The maximum pressure on the contact point
k_o	Stiffnes of contact wire
C	Contact wire wave propagation speed
P_o	Pantograph force on contact wire (at rest)
P	The contact force on the contact wire at different speed of train
d_{up}	Maximum contact wire uplift at steady-arm
λ	Eigen value
∇	Maximum pantograph vertical amplitude
NQ	Percentage of real arcing
c_b	Coefficients of minor ellipse axis
c_δ	Coefficient of compressive stress
c_d	Coefficient of deformation
c_τ	the coefficients of shear stress
K	the ratio of the minimum to the maximum axis of the ellipse
C_z	The coefficient for the displacement in z direction
τ_{max}	The maximum shear stress
EN	European norm
RTRI	Railway Research Department in Japan.
OCL	Overhead Contact Line
LN_1	Catenary with stitch wire
LN_2	Catenary without stitch wire

K_{Lc}	Elasticity constant of the contact line
Y_{LC}	Displacement of contact wire in the direction of Y axis
A	Constant of the functions of the four principal radii of curvature.
B	Constant of the functions of the four principal radii of curvature.
a	Semi major axis of the contact ellipse.
b	Sminor axis of the contact ellipse.
ν	Poisson's ratio
σ_c	Maximum compressive stress
σ_{ys}	Yield strength in tension
τ_{max}	Maximum shear stress
σ_x	Stress in the x-direction
σ_y	Stress in the y-direction
σ_z	Stress in the z-direction
$A_1, A_2, B_1, B_2, C_1, C_2$	Constant coefficients

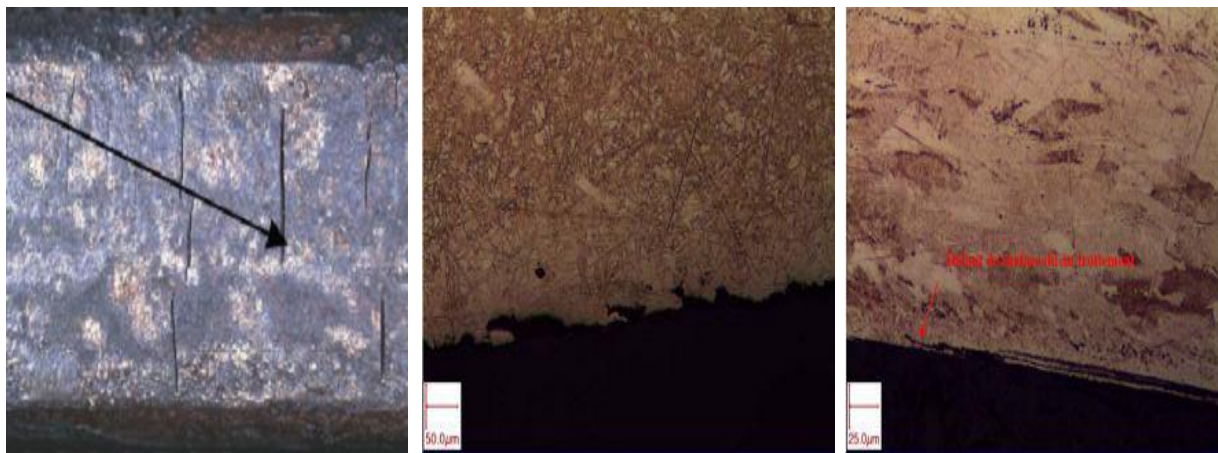
CHAPTER ONE

INTRODUCTION

1.1. Back ground of research

The system that supplies electricity to trains is called catenary– pantograph system ;(see figure 2) .It mainly consists of the contact wire, messenger wire and the pantograph. On top of the train sits the pantograph that slides along the contact wire collecting electrical power and delivers it to the train’s motor. Contact between the pantograph and the contact wire is an important measure of current collection performance; it is described by a dynamic contact force. Either too low or too high contact force yields fatigue fracture effect on the system.

The fatigue fracture is one of the most critical failures which occur on the rail way network, because it is undetectable and it has a huge impact on traffic disruption. The defects occur in the contact wire surface due to pantograph friction, electrical arcs, Corrosion and cyclic load which leads crack initiation are seen in figure 1a, b & c [1].



a)

b)

c)

Figure 1: Contact wire surface defects due to, electrical arcs, Corrosion and cyclic load [1].

- a) (left) Crack initiations and surface defects in the contact wire;
- b) (centre) micrographic section of the contact wire: specks due to electrical arcs;
- c) (Right) micrographic section of the contact wire: surface defects due to friction.

The aim of this thesis is to predict fatigue failure of railway contact wire system. The parameters which affect the system are wave propagation velocity in the contact wire, pre-sag of the system, tension in the wires and material property of the contact wire.

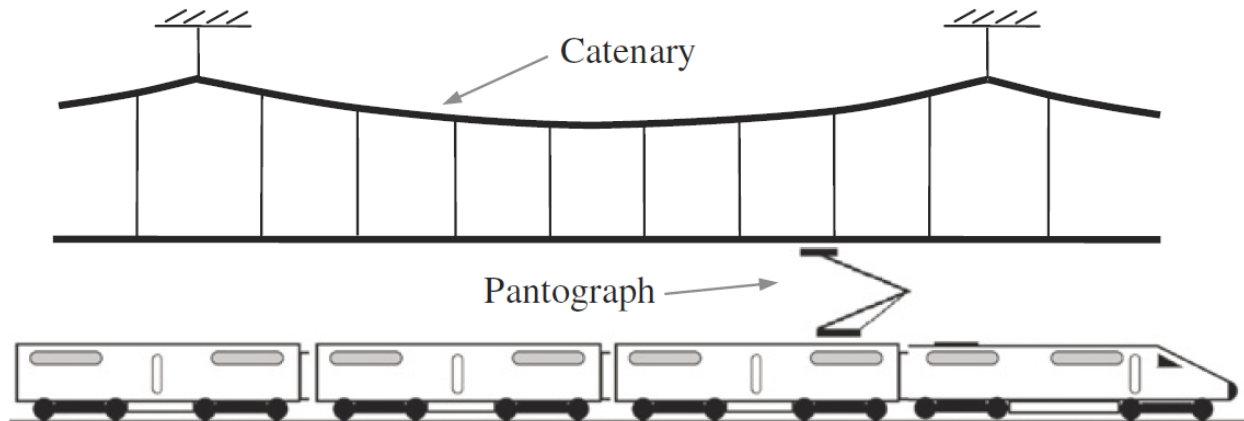


Figure 2: Pantograph-catenary system [2]

1.2. Different catenary systems

There are three typical types of catenary systems (a) simple catenary (b) stitched catenary (often referred to as Y-line) and (c) compound catenary

These three types can further more be divided according to the method of producing tension in the wires. Either the wires are fixed at the support poles or weight-tensioning devices are used. If the wires are fixed, pre-sag and tension vary with temperature and therefore it is considered inconvenient for high train velocity (Farr et al., 1961) [2].

The simple catenary arrangement was among the first systems to supply electric power to running trains. Its disadvantage is the large stiffness variation along the span, yielding more dynamic effects in the system because the pantograph will lift the wire higher in the middle of the span than at the supports. Ideally the vertical height of the pantograph should be uniform as it runs through, to do that the system's stiffness variation must be as small as possible. To counteract this problem, the stitched and compound catenary systems were developed. The stitched catenary is supposed to smooth out the irregularity of the stiffness at the supports. That is accomplished by supporting the contact wire with an additional wire, see figure [3]. Stitched

catenary systems are also commonly used to increase performance of tracks that run in a curvature.

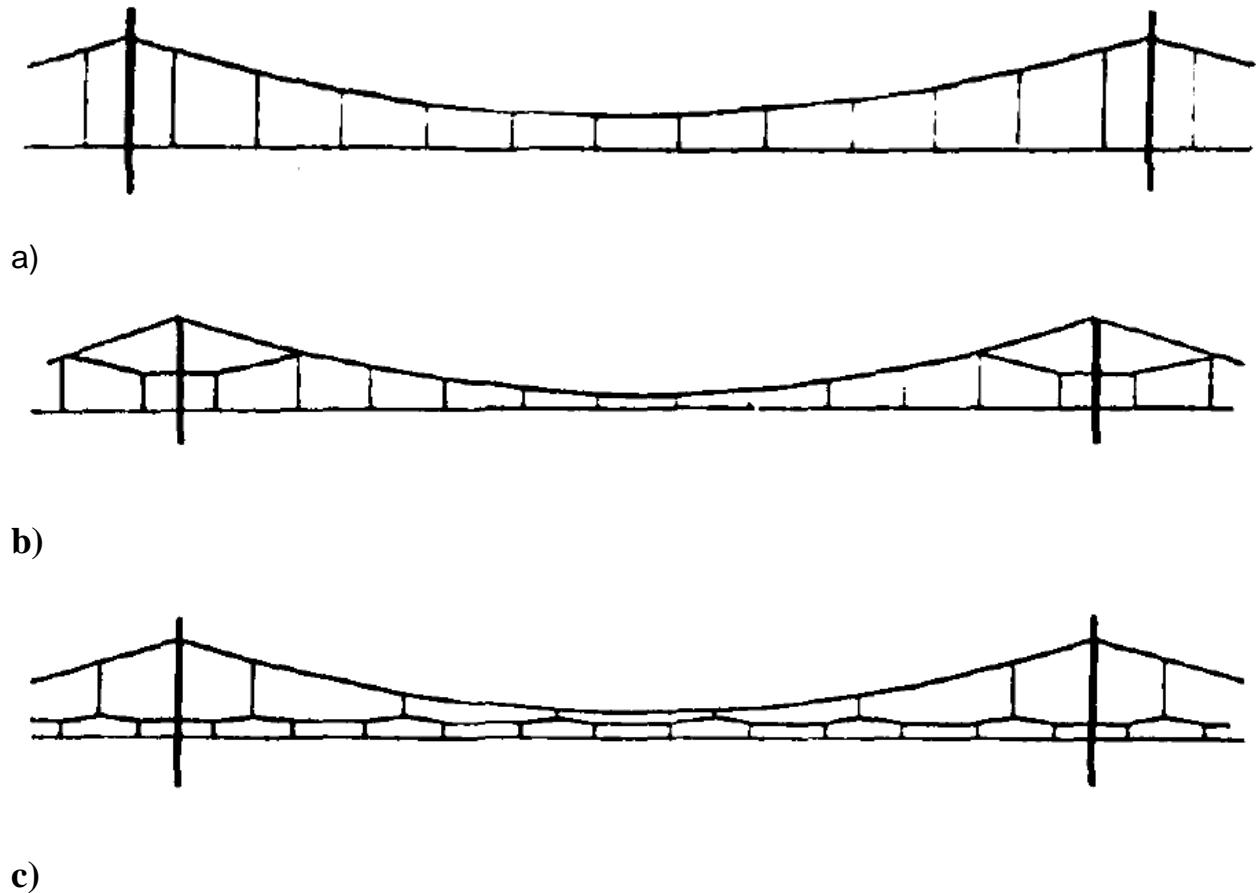


Figure 3: Different catenary structures (a), stitched catenary (b) (often referred to as Y–line) and (c) compound catenary [2].

1.3. Statement of the problem

In today's, railway technologies pantograph-catenaries system is subjected to fatigue failure which occurs unexpectedly and results interruption of transportation (discomfort to passengers and economical problem to railway industries). Thus, researches now try to focus on pantograph-catenary fatigue life.

1.4. Significance of the research

This paper is significant for railway organizations in predicting the contact wire fatigue life. By doing so they can increase the life time of the catenary system which is expensive, minimizes delays to passengers' transportation. Generally it maximizes the profitability of the organization.

1.5. Objective of the research

1.5.1. General objective of the research

Developing pantograph-catenary contact and predicting fatigue failure of contact wire (catenary) of railway.

1.5.2. Specific objective of the research

- Predicting the contact wire fatigue life via ANSYS soft ware.
- Analytical analysis of pantograph-catenary contact.
- Comparing the results with experimental results.
- Comparing the results on the contact wire, when there is a dropper and away from the dropper.

1.6. General methodologies

The methods used are;

- Analytical analysis of pantograph-contact wire.
- Modeling pantograph-contact wire via ANSYS soft ware.
- Finite element analysis by ANSYS finite element soft ware.
- Fatigue life analysis through ANSYS soft ware and comparing the result with experimental results carried out in rail way organizations which are published in Journals.

1.7. General conditions

- Considering both the lower and upper arm are fixed and vertical motion is results from motion of the pantograph slipper.
- The lateral movement of the pantograph-catenary is neglected.
- The vertical motion is assumed as periodical $P(t) = P_o - A\sin(\omega t)$ with amplitude A and deflection in the direction of Y axis.

1.8. General parameters

- Parameters of over head contact wire [13].

Parameters	Values
Contact wire tension	12kN
Contact wire density	$0.987\text{Kg}\text{m}^{-1}$
Contact wire flexural rigidity EI	130Nm^2
Span length	30m
Coefficient of expansion	$17 \times E^{-6}$
Nominal cross section area	120mm^2
Tensile strength	$350\text{N}/\text{mm}^2$

CHAPTER TWO

LITERATURE REVIEW

2.1. Introduction

The Overhead Conductor System (OCS) is installed above and along the railway tracks and interfaces with the collection strips of train pantographs to provide the electric energy to trains and generate traction motive forces.

The catenary–pantograph is subjects to abrasion, fatigue, friction, scraping, corrosion, erosion, vibration, arcing and welding at different degrees of severity depending on the wire and collector strip materials, modes of interaction and the environmental conditions. Similarly external influences such as wind (to induce wire galloping) and humidity can have an effect on the rate of contact wire wear. There are many researchers who have conducted for rail way transportation. Their purposes are to find and determine the factors that lead to early failure of pantographs and contact wire by using various techniques to model the catenary-pantograph contact and predicting of the contact (catenary) fatigue failure by doing so the rail way maintenance cost and down time will be minimize. Hence, the rail way organizations will be profitable, the society will get enough transportation and concurrently the economy of the country will grow up.

Among the different researches carried out on the development of pantograph-catenary contact and predicting the life of the catenary are;

- 1) Fatigue Life Prediction Method for Contact Wire Using Maximum Local Stress.
- 2) Dynamic behavior of contact lines for railways with laboratorial model setup according to Norwegian conditions.
- 3) Analysis of the “Catenary - Pantograph” assembly’s dynamic behavior by numerical-simulation.
- 4) Wave propagation in a catenary system for a high-speed railway.
- 5) Reliability analysis of TSG19-type pantograph based on time-dependent parameters
- 6) Development of Multibody Pantograph and Finite Element Catenary Models for application to High-speed Railway Operations.
- 7) Fatigue analysis of catenary contact wires for high speed trains.

- 8) A Survey of Contact Wire Wear Parameters and the Development of a Model to Predict Wire Wear by using the Artificial Neural Network.
- 9) Conducted and Radiated Electromagnetic Interference in Modern Electrified Railways with Emphasis on Pantograph Arcing.

The paper on the “Fatigue Life Prediction Method for Contact Wire Using Maximum Local Stress” suggests the fatigue life evaluation method for contact wire using an ASTM E466 standard specimen [1]. First, a standard fatigue test is performed on pure copper, which is used for 300 km/h trains in Korea. In addition, the fatigue life prediction equation (vs. uplift amount), which can predict fatigue life determined from a structure test using standard specimen test results, was employed. Finally, the predicted life from the suggested equation is compared with the results of structure tests by Kang et al. for verification.

The bending fatigue life of a contact wire structure was predicted using the stress-strain relation obtained from a tensile test of the specimen and the local stress-uplift amount relation obtained from the contact wire structure. In addition, a fatigue life prediction equation which can predict the fatigue life of a contact wire structure using standard specimens is suggested for the 300 km/h-level contact wire used in Korea. Thus, the paper predicts the fatigue life of a contact wire structure using the maximum local stress at the top of the contact wire caused by uplift force [4].

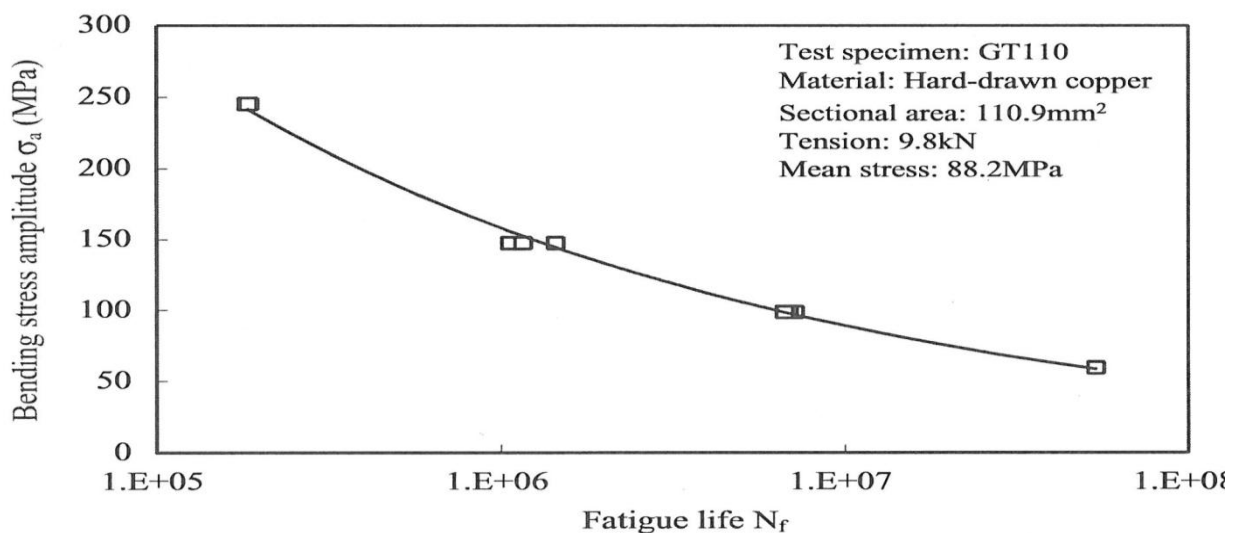


Figure 4: Bending stress vs fatigue life of contact wire

The research [1] limitation is

- It is not assisted with soft ware simulation.

The research on;

“Dynamic behavior of the catenary–pantograph system has been examined, by a literature survey and by modeling it numerically.” [2]. The main critical considerations taken for the dynamic behavior of the catenary system are wave propagation velocity, speed of the train, limiting speed due to reflection in the system and the critical damping ratio.

Parameters of the system controlling the first two properties are tension in the wires and their mass per unit length. Wave propagation velocity proved to be a critical factor to the system; it is controlled by mass per unit length and tension force in the wire. Behavior of the system becomes chaotic as the train’s speed nears this velocity limit and the parameters controlling it should be set so that the limit is high. The further the train’s velocity is from the wave propagation velocity, the better the system behaves. The Same effects were observed when the velocity of the train was around the limiting speed due to reflection in the system.

The other research carried out on the topic, “Dynamics and Control of a High Speed Train Pantograph System”[5], in this work it wasn’t only intended to study a pantograph for high speeds but to study the feasibility of using in standard train speed lines, controlled pantograph. The inclusion of control in pantograph systems cannot only be associated to decreasing the travel time between destinations; it has a more brooder area of influence. Pantograph systems have typically low maintenance, but this machine is an expensive component of the train, due to its robustness to sustain physical contact with the wires and to resist to bad weather conditions and electric arc formations. Traditional approaches (with no control) resort to aerodynamic wings in the registration strip. Good results have been obtained resorting to this technology using the air lift that raises the registration strip with higher train velocities ensuring better contact at high speeds. But excessive wear to the interface elements still occur and pantograph fixation to the cable system are still present. Evolving to systems that have very low wear to the pantograph and catenary, that have very low maintenance and have minimum risk of pantograph fixation to the cable system is a very appealing solution for every train transportation company.

If improvements are to be made for the model [2] in the future

- It is important that these characteristics should not be lost. The ideas for future work improvements on the model are presented given that criteria. If these improvements yield increased complexity in the model and a long calculation time it would perhaps be better to turn to commercial finite element software such as ABAQUS or ANSYS.
- Changing the model from 2D to 3D would allow for effects such as curvature and zig-zag to be included. These effects are important to the system's behavior and should be included, but it would be risky since the calculation time could increase.
- Adding nonlinear effects of dropper slackening. Many studies have shown the importance of this property to the systems behavior and adding it should be included (Cho, 2008). That would mean that for every time step the geometry of the droppers need to be checked and if they are in compression the global stiffness and damping matrices need to be updated. This operation could be time consuming, but since the matrices in whole are not being changed, this could be a possibility for improvement.
- Changing the program code so that spans of different lengths and with different dropper arrangement could be modeled together. In reality different span arrangements are often built side by side and full-scale measurement data does exist for these lines that could be used for validating the model. Validation is possible for the model as it is today but this could give more accuracy in the results. This improvement would not result in increased calculation time.
- Implementing the option of having multiple pantographs. If damping is to be studied for the system, including multiple droppers is essential. Damping does not affect the system to a great degree when there is only one pantograph. Increase in calculation time should not be significant, and for simplicity the same mathematical model could be used for both pantographs.
- Different contact formulation methods should be tested. The one used in this thesis proved successful, but there are many formulations that have been implemented and it would be interesting to see if any of them gives better results.
- Making the computer code more user friendly, i.e. commercializing it. Setting up a simple graphical user interface could make the model more accessible.

Checking dynamic performances of a system with a model that requires only minutes in calculation time and can easily change system parameters is good to have.

The research on “wave propagation of catenary system in high-speed railway” [6]. The dynamic and static behaviors of a three-dimensional linear catenary system for a high-speed railway are analyzed by using the finite element method. Considering tensions in the contact wire and the messenger wire, it tries to drive the equations of motion for the three-dimensional catenary system. These equations are for the longitudinal, transverse, vertical and torsional motions. In other words, each node has six degrees of freedoms: translation and rotation motion in x , y and z directions in Cartesian coordinate. After establishing the governing equations, the weak forms are spatially discretized with two-node beam elements. With the discretized equations, a finite element computer program is developed for the static and dynamic analyses. The static deflections are computed when the gravity and tension are applied in contact and messenger wires. Also, the slackness of the dropper which has a geometry nonlinear effect is also considered in the static and dynamic analyses. The slackness of the dropper is an important phenomenon, because the wave propagation and the wave reflection in the catenary are influenced by the slackness. The contact force between catenary and pantograph are determined by wave propagation and reflection. Finally, the dynamic responses of the system are also investigated when applying a load to the contact line. For confirmation of the wave propagation and the reflection, we model the applied load as the point mass. Then, we calculate the contact force between the catenary and the point mass when the velocity of the point mass is zero, and compared the theoretical wave speed with the simulation result by observing the variation of the contact force [6].

Limitation of the study [6]

- The research did not consider the effect of fatigue on the contact wire.
- It did not consider experimental results carried out.
- Here, the effect of friction is neglected.
- It did not consider the effect of droppers on the fatigue failure of the contact wire and without them.

The research carried on “Reliability analysis of TSG19-type pantograph based on time-dependent parameters” shows a method to test the collectors damping in a TSG19-type pantograph and a model to predict and calculate the life of damaged upper arms based on time-dependent parameters [7].

The present study showed clearly that a formation of a premature crack at the upper arms is due to high values of stress at the critical section of upper arms. Furthermore, an inspection of the pantograph of high-speed vehicles running in the main line also showed that the collector spring was damaged. This lead to a degeneration of the spring parameters, mainly an increase of the stiffness of the first mass and to a decrease of the damping as mileage increased. The root cause of the crack in the upper arm is that the stiffness of the collector spring increased at the same time that the damping of the collector’s spring decreased as running mileage increased. However, the design modification of the collector spring may have aggravated such damage.

The contact force between catenary and pantograph increased when time-dependent parameters of the first mass were considered, which modified the catenary–pantograph dynamic model. With higher contact forces, amplitude and cycles of dangerous stress also increased.

A proper lifetime prediction of the upper arm showed that time-dependent parameters of pantograph led to shorter values of the upper arm life time.

The research performed on Fatigue analysis of catenary contact wires for high speed trains [9] is one of the most critical failures which may occur on the high speed network because it is undetectable and it has a huge impact on traffic disruption, client discomfort (delays, speed slowdowns) and cost explosion. Unfortunately, conditions of use increase the risk of fatigue failure:

In France, some fatigue failures has already occurred on the overhead contact line between Paris and Lyon [1]. This overhead line was replaced after only 29 years of use because fatigue failures took place under the junction claws. This component, commonly used in maintenance on classical lines, appeared to be inadequate when used on high speed lines. Its heavy weight and its high stiffness produce important dynamic loads and arcing with the pantograph passage [1]. A modification of the maintenance procedure limits the number of settled claws and their duration, but the fatigue could take place on other lines.

Indeed, the French network speed rising tendency requires an increase of the mechanical tension in the contact wire and this parameter heightens the fatigue failure phenomenon.

The RTRI research department built a specific test bench to study fatigue breakage phenomenon [8]. This test bench described in the Figure 4 was designed to reproduce realistic operation conditions by using a sample of real contact wire, by adding a tensile load on the contact wire to obtain the relevant mean stress and by applying a representative bending stress controlled by deformation. Considering the test is performed on a sample of a real contact wire, without any machining and thus with a constant section, a three bending point bench was chosen to force the fatigue failure to take place under the oscillating roller as described in Figure 5. In this way, it is easier to stick sensors close to the crack initiation point.

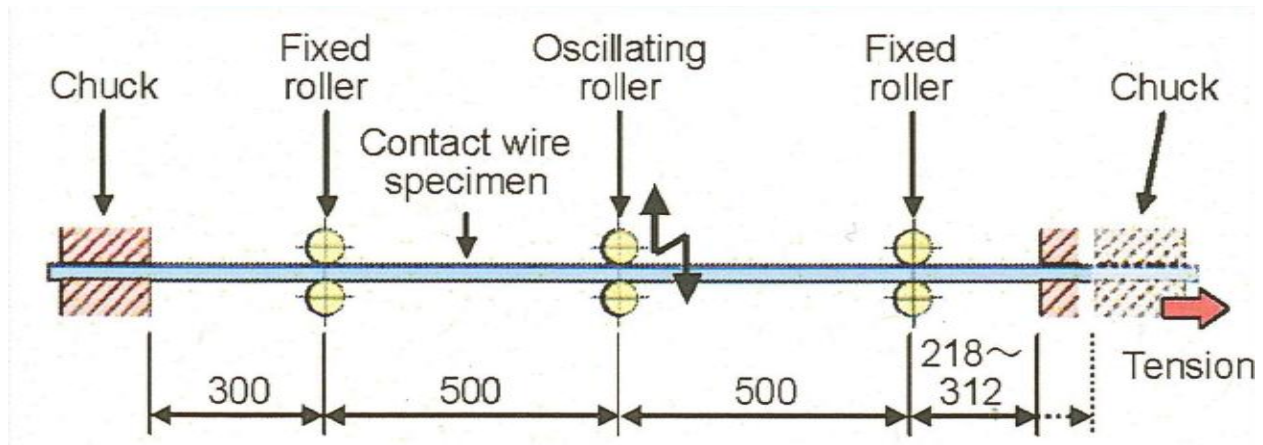


Figure 5: RTRI test bench for over head contact wire study [1]

The fatigue crack appearance is shown in Figure 6. The three steps of the fatigue process can be identified: crack initiation, crack propagation and failure. The origin of the fatigue crack occurred on the top of the contact wire. Indeed, a dark area corresponding to crack initiation begins on the upper edge of the wire and the crack propagates to failure by necking of the wire. One can note that these tests are reproducible and evolution of the fatigue fracture appearance remains independent of the bending strain amplitude.

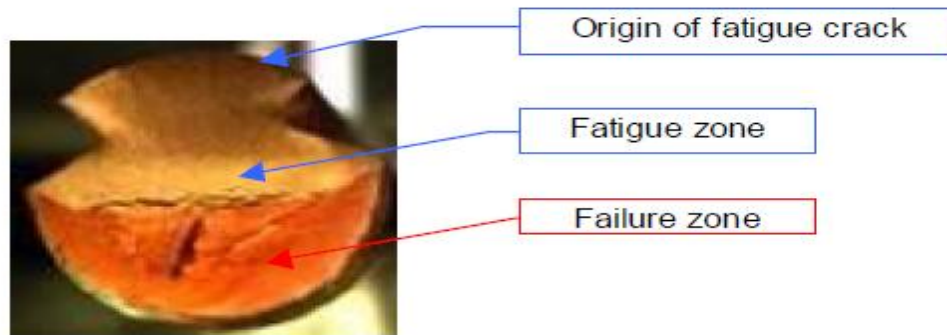


Figure 6: Fatigue fracture obtained on the RTRI's bench [9].

Limitation of the study (for future work) [9]

- ❖ The research considers the French railways as a model.
- ❖ The research did not develop the contact between the pantograph-catenary system and it did not consider the life span of the contact wire.
- ❖ It did not consider the effect of droppers on the fatigue failure of the contact wire and without them.
- ❖ The effect of friction is neglected.

The research on “A survey of contact wire wears parameters and the development of a model to predict wire wear by using the artificial neural network” [10] deals on the contact wire wear and it stated that if the contact wire is worn below its limit then the electrical resistance may result in a voltage drop becoming too high and train motors may stall and burn out. If the contact wire fails mechanically i.e. below the minimum tensile strength, then it may break due to tension on the wire. Without a creditable method of predicting the condition of the contact wire then it would eventually reach the threshold and place the system at risk of a failure. The railway operator needs to be proactive and prudent in the planning and executing a wire replacement program, well before the wire reaches its engineering limits or a failure that can drain resources unnecessarily [10].

Table 1 : Material composition of contact wire

	Contact wire EN 50149		
Major elements	copper alloy CuAg 0.1	Cu	99.88-99.91%
		Ag	0.09-0.12%
Nominal cross sectional area	120mm ²		
Nominal mass	1070kg/m		
Modulus of elasticity	12.4*E4N/mm ²		
Tensile strength	350N/mm ²		
Coefficient of expansion	17*E-6		

The research carried on “Conducted and Radiated Electromagnetic Interference in Modern Electrified Railways with Emphasis on Pantograph Arcing” [11] focuses on sliding contact between the pantograph-catenary systems, while transmitting electrical power to the motors.

2.2. Requirements of a pantograph-overhead wire while sliding contact

The contact area between the overhead contact wire and the carbon blade of the pantograph is of the order of square mm, through which several MW of power are transmitted. Depending on the voltage levels, sometimes more than 1000 A current flows through this small contact area. To achieve this and also provide quality power to the propulsion system requires smooth operation of the sliding contact and so, it should have the following properties: [11]

- ❖ The physical contact between the pantograph and the overhead contact wire must be maintained continuously as the train moves
- ❖ The pantograph must provide low aerodynamic resistance
- ❖ The wear of the carbon blade should be low
- ❖ The overhead contact wire should not be abraded

Both the pantograph and the overhead contact wire should be able to withstand high current and high temperature

- ❖ Even when the train is stationary, it still draws some power (80-300 A, depending on supply voltage as per IEC 50367:2006) and the contact should be able to bear that without being welded/joined

2.3. Material perspective

Pure carbon is still being used in many railways for pantograph. [2] Since only one blade is used in most of the high speed railways, the current density is very high in the contact region. This can cause increased wear of the overhead contact wire as well as contact strip surface, where metal migration occurs during arcing. Another issue is the increase in temperature when the train is at standstill and still drawing current. This is due to increased resistivity of the contact surface by metal migration

The Limitation of the study [11]

- The study focuses on the electrical arcing caused on the contact between the pantograph-catenary systems due to lose of contact.
- It does not consider the effect of cyclic load on the system.
- It does not develop the contact point between the pantograph-catenary systems based on contact mechanics.
- It does not consider the effect compressive stress of the pantograph-on the contact wire.

CHAPTER THREE

ANALYSIS OF PANTOGRAPH CATENARY INTERACTION

3.1. Material selection of catenary wire

When selecting catenary wire material, two main concerns need to be addressed, the line tension and the dropper slacking. The line tension on a catenary is often employed by means of weights or occasionally by hydraulic tensioners. In either case the method ensures that the line tension on the catenary wires, respectively the contact wire and the messenger wire, are kept under a constant tension as much as possible considering temperature changes.

	Material	Density/ ($\text{kg}\cdot\text{m}^{-1}$)	Tension/KN	Section area/ mm^2
Contact wire	CTMH-150	1.35	28	150
Support wire	JTMH-120	1.07	23	120
Assistant wire	JTMH-35	0.31	3.5	35

	Contact wire	Messenger wire	Droppers	
Section(mm^2)	150	65.5	12	
Mass(Kg/m)	1.334	0.605	0.11	
Young modulus(Gpa)	120	84.7	84.7	
Tension(N)	20000	14000	-	
Claw Mass(kg)	0.195	0.165	-	

Table 2 : Material property of LN2 catenary wire [12]

	Contact wire	Messenger wire	Droppers	
Section(mm ²)	150	117	12.6	
Mass(Kg/m)	1.335	1.0378	0.1173	
Young modulus (Gpa)	100	96.8	15.9	
Tension(N)	20000	16000	-	
	0.195	0.165	-	

Table 3 : Material property of C270 catenary Wire [12]

	Contact wire	Messenger wire	Droppers	
Section(mm ²)	120	120	12.6	
Mass(Kg/m)	1.075	1.068	0.086	
Young modulus(Gpa)	120	84.7	84.7	
Tension(N)	27000	21000	3500	
Claw Mass (Kg)	0.25	0.25	-	

Table 4 : Material property of Re330 catenary [12]

❖ For this thesis it is taken the standard parameters of over head catenary system

	Material	Density/ (kg.m ⁻¹)	Tension/KN	Section area/mm ²
Contact wire	CTMH-150	0.981	12	150
Support wire	JTMH-120	1.07	10	120
Assistant wire	JTMH-35	0.31	3.5	35
Contact wire flexural rigidity EI=(130Nm ²)				

Table 5 : Materials and structure of the catenary [13]

3.1.1. Material selection for Pantograph

Carbon is used material in overhead sliding contact (pantograph), but it was not used in the former Japanese National Railway (JNR) being its low mechanical strength and high electrical resistivity did not match their requirements. Instead sintered metal alloys were preferred, including the Shinkansen for almost decades. Later to decrease the wear of the contact wire, carbon contact strips with electrical resistivity less than 3Ω were developed which started replacing the sintered metal alloys by late eighties [14,16]. Carbon, Sn-Sb alloy impregnated carbon, Cu or Cu alloy impregnated carbon are the most widely used material for sliding contact. While pure carbon is still being used in many railways, Cu or Cu alloy impregnated carbon is most popular in many railway organizations [15, 16]. Hence, in this research carbon is taken as material for pantograph.

3.1.2. Numerical Analysis

Assumptions:

- Considering both the lower and upper arm are fixed and vertical motion is results from motion of the pantograph slipper in constant contact between pantograph-over head contact wire.
- The lateral movement and aerodynamic effect on the pantograph-catenary is neglected.
- The vertical motion is assumed as periodical $P(t) = P_o - A\sin(\omega t)$ with amplitude A and deflection in the direction of Y axis.
- Span length of catenary system $L=30\text{m}$
- M_p Pantograph mass;
- μ Coefficient of the pantograph;
- K_a The elasticity constant of the pantograph's spring considered constant;
- F_{fp} The friction forces into the joint of the pantograph considered constant;
- K_{lc} The elasticity constant of the contact line;
- Y_{lc} The displacement of the contact line in the y direction;
- Y_s The distance between the catenary wire and the pantograph is considered zero;

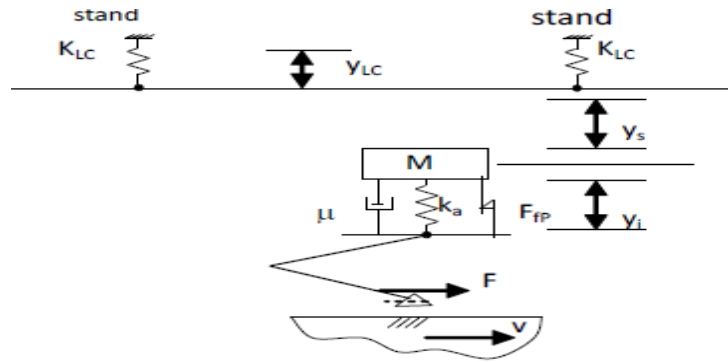


Figure 7: Model of Pantograph-Catenary [17]

The excitation force of the system is given by

$$P(t) = P_o - A\sin(\omega t) \dots\dots\dots 3.1$$

Where,

- P_o is the force which assures the contact between the pantograph and the contact line.
- ω is the frequency of the system, which is dependent on the speed of the train and the length of the span.
- A is the double amplitude of the vertical motion of the pantograph.

To analyze the frequency(ω) of the catenary (contact) wire ,it is necessary to consider the dynamic interaction between a rigid mass m moving with constant speed V along a simply supported beam as it is reviewed ad investigated by **Manson** .(length L ,mass per unit length m ,bending stiffness EI was examined as

$$\frac{V}{V_{ref}} = 0.5 \text{ were used and the referance speed } V_{ref} = 2L/T_e \text{ [18]}$$

and $T_e = \frac{1}{f_e} = 2\pi/\omega_e \dots\dots\dots 3.2$

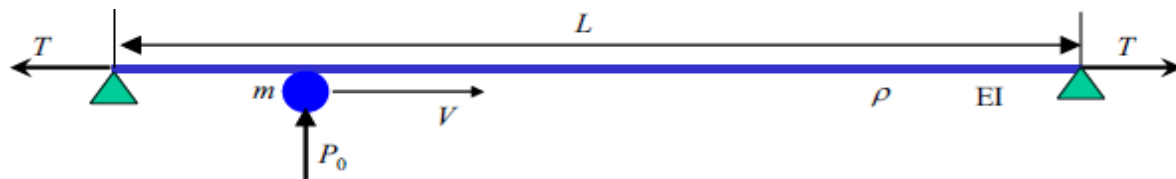


Figure 8: Model of catenary system as beam element [10]

Where,

T_e : The Eigen period (cycle)

ω_e : Fundamental Eigen Frequency.

By considering the different speed of the train, we can find the driving frequency of catenary (contact wire)

Case I

- For train speed of 50km/hr and length of span length of 30m.

$$\frac{50\text{km}}{\text{hr}} * \frac{10}{36} = 13.9\text{m/s}$$

$$V_{\text{ref}} = \frac{V}{0.5} = \frac{13.9}{0.5} = 27.77$$

$$V_{\text{ref}} = \frac{2L}{T_e} \Rightarrow T_e = \frac{2L}{V_{\text{ref}}} = 2 * \frac{30}{27.77} = 2.16$$

$$T_e = \frac{1}{f_e} = \frac{2\pi}{\omega_e} \Rightarrow \omega_e = \frac{2\pi}{T_e} = \frac{2\pi}{2.16} = 2.9\text{Hz.}$$

Case II

- For train speed of 60km/hr and length of span of 30m.

$$\frac{60\text{km}}{\text{hr}} * \frac{10}{36} = 16.667\text{m/s}$$

$$V_{\text{ref}} = \frac{V}{0.5} = \frac{16.667}{0.5} = 33.33$$

$$V_{\text{ref}} = \frac{2L}{T_e} \Rightarrow T_e = \frac{2L}{V_{\text{ref}}} = 2 * \frac{30}{33.33} = 1.8$$

$$T_e = \frac{1}{f_e} = \frac{2\pi}{\omega_e} \Rightarrow \omega_e = \frac{2\pi}{T_e} = \frac{2\pi}{1.8} = 3.49\text{hz.}$$

Case III

- For train speed of 70km/hr and length of span of 30m.

$$70 \frac{\text{km}}{\text{hr}} * \frac{10}{36} = 19.44\text{m/s}$$

$$V_{ref} = \frac{V}{0.5} = \frac{19.44}{0.5} = 38.89$$

$$V_{ref} = \frac{2L}{T_e} \Rightarrow T_e = \frac{2L}{V_{ref}} = 2 * \frac{30}{38.89} = 1.54$$

$$T_e = \frac{1}{f_e} = \frac{2\pi}{\omega_e} \Rightarrow \omega_e = \frac{2\pi}{T_e} = \frac{2\pi}{1.54} = 4.08 \text{ Hz.}$$

No.	Speed of train(km/hr)	Driving frequency of catenary (hz.)
1	50	2.9
2	60	3.49
3	70	4.08
4	278	16.173

Table 6 : Relating Speed of the train and driving frequency of contact wire

3.2. Determining the contact force using European standards

The types of high-speed catenaries existing today in different countries are either simple, stitch wire or compound catenaries. The trend of new implementations of high-speed lines is to use simple catenaries. But the need for increasing the train operating velocities not only forces that limits the speed and also the catenary designs to present a smoother geometry of the contact wire, while maintaining a flexibility as constant as possible, withstand higher tension forces on the messenger and contact wires.

One of the critical parameters that limits the operational velocity of the trains is the wave propagation velocity on the contact wire, C , [19]

$$C = \sqrt{\frac{\pi^2 EI}{\rho L^2} + \frac{T}{\rho}} \dots\dots\dots 3.3$$

Where T is the tension of the contact wire, ρ is the contact wire mass per length unit, EI is the beam bending stiffness and L is the beam length. When the train speeds approach the wave propagation velocity of the contact wire, called critical velocity, the contact between the

pantograph and the catenary is harder to maintain due to increase in the amplitude of the catenary oscillations and bending effects. In order to avoid this deterioration of the contact quality the train speed should not exceed 70-80% of the contact wire wave propagation speed

[20]. for safety the maximum train operating speed, V , is set to be $V=0.7C$.

When modeling catenary systems, two main concerns need to be addressed, the line is tensioning and the dropper slacking. The line tension on a catenary is often employed by means of weights or occasionally by hydraulic tensioners. In either case the method ensures that the line tension on the catenary wires, respectively the contact wire and the messenger wire, are kept under a constant tension as much as possible considering temperature changes. To apply the tension on the wires by weights a pulley system is mounted on both end supports of the catenary where the wires meet and a set of weights hangs as represented on figure 22.

The quality of the pantograph-catenary contact required for train speed operations is quantified in current regulations (EN50317, 2012; EN50367, 2006). The norm EN50367 specifies the following thresholds for pantograph acceptance (EN50367, 2006)

- Mean contact force (P) $P= 0.00097v^2 + 70N$
- Standard deviation (δ_{max}) $\delta_{max} < 0.3Fm$
- Maximum contact force (F_{max}) $p_{max} < 350N$
- Maximum CW uplift at steady-arm (d_{up}) $d_{up} = 120mm$

$$C = \sqrt{\frac{\pi^2 EI}{\rho L^2} + \frac{T}{\rho}}$$

Where, $T = 12000N$, $EI = 130$, $\rho = 0.981kg/m^{-1}$, $L = 30m$, and $\pi = 3.14$ [13]

$$C = 110.606 m/s = 398.18 km/hr.$$

Therefore, the maximum operating speed of the train is

$$V = 0.7C = 0.7(398.18) = 278.726 km/hr.$$

- For Ethiopian rail way trains running speed.

For speed of 50 km/hr

$$P = 0.00097v^2 + 70 = 72.425N$$

For speed of 60 km/hr

$$P = 0.00097v^2 + 70 = 73.492N$$

For speed of 70 km/hr

$$P = 0.00097v^2 + 70 = 74.753N$$

But, the catenary system can allow up to speed of 278km/hr and the mean contact force is

For speed of 278km/hr

$$P = 0.00097v^2 + 70 = 145N$$

Speed of train (km/hr.)	50	60	70	278
Contact force (N)	72.425	73.492	74.752	145

Table 7 : The contact force for different speed of trains

3.3. Calculating the natural frequency of the system

At high speeds the quality of the contact depends only on the dynamics of the pantograph and catenary. An important characteristic is the resonance phenomenon which consists in larger amplitude of the pantograph oscillations to the values that can produce a detachment of the slipper from the contact line. The critical phenomenon for cause of resonance is when the natural frequency of the object and the driving frequency are nearly equal.

We need to check the natural frequency of the catenary system, by assuming as a beam element and the finite element equations of motion for a beam element are

$$[m^{(e)}] \begin{Bmatrix} \ddot{v}_1 \\ \ddot{\theta}_1 \\ \ddot{v}_2 \\ \ddot{\theta}_2 \end{Bmatrix} + [k^{(e)}] \begin{Bmatrix} v_1 \\ \theta_1 \\ v_2 \\ \theta_2 \end{Bmatrix} = - \int_0^L [N]^T q(x, t) dx + \begin{Bmatrix} -V_1(t) \\ -M_1(t) \\ V_2(t) \\ M_2(t) \end{Bmatrix} \dots\dots\dots 3.4$$

The consistent mass matrix for a two-dimensional beam element is given by

$$[m^{(e)}] = \rho A \int_0^L [N]^T [N] dx \dots\dots\dots 3.5$$

Substitution for the interpolation functions and performing the required integrations gives the mass matrix as

$$[m^{(e)}] = \rho AL/420 \begin{bmatrix} 156 & 22L & 54 & -13L \\ 22L & 4L^2 & 13L & -3L^2 \\ 54 & 13L & 156 & -22L \\ -13L & -3L^2 & -22L & 4L^2 \end{bmatrix}$$

The assumption for the catenary is as a beam element which is fixed at both ends and consider the force is applied at center of the beam. Then, we will divide the beam as two sections, one element from one end to the center and the other is from center to another end.

Element mass matrix of first element

$$m_{11} = \rho AL/420 \begin{matrix} & v_1 & \theta_1 & v_2 & \theta_2 \\ \begin{bmatrix} 156 & 22L & 54 & -13L \\ 22L & 4L^2 & 13L & -3L^2 \\ 54 & 13L & 156 & -22L \\ -13L & -3L^2 & -22L & 4L^2 \end{bmatrix} \end{matrix}$$

$$m_{21} = \rho AL/420 \begin{matrix} & v_2 & \theta_2 & v_3 & \theta_3 \\ \begin{bmatrix} 156 & 22L & 54 & -13L \\ 22L & 4L^2 & 13L & -3L^2 \\ 54 & 13L & 156 & -22L \\ -13L & -3L^2 & -22L & 4L^2 \end{bmatrix} \end{matrix}$$

Global stiffness matrix

$$M = \rho AL/420 \begin{bmatrix} v_1 & \theta_1 & v_2 & \theta_2 & v_3 & \theta_3 \\ 156 & 22L & 54 & -13 & 0 & 0 \\ 22L & 4L^2 & 13L & -3L^2 & 0 & 0 \\ 54 & 13L & 312 & 0 & 54 & -13 \\ -13L & -3L^2 & 0 & 8L^2 & 13L & -3L^2 \\ 0 & 0 & 54 & 13L & 156 & -22L \\ 0 & 0 & -13L & -3L^2 & -22L & 4L^2 \end{bmatrix}$$

Element stiffness matrix of first element

$$K_{11} = \frac{EI}{L^3} \begin{bmatrix} v_1 & \theta_1 & v_2 & \theta_2 \\ 12 & 6L & -12 & 6L \\ 6L & 4L^2 & -6L & 2L^2 \\ -12 & -6L & 12 & -6L \\ 6L & 2L^2 & -6L & 4L^2 \end{bmatrix}$$

For the second element

$$K_{21} = \frac{EI}{L^3} \begin{bmatrix} v_2 & \theta_2 & v_3 & \theta_3 \\ 12 & 6L & -12 & 6L \\ 6L & 4L^2 & -6L & 2L^2 \\ -12 & -6L & 12 & -6L \\ 6L & 2L^2 & -6L & 4L^2 \end{bmatrix}$$

For Global stiffness matrix

$$K = EI/L^3 \begin{pmatrix} v_1 & \theta_1 & v_2 & \theta_2 & v_3 & \theta_3 \\ 12 & 6L & -12 & 6L & 0 & 0 \\ 6L & 4L^2 & -6L & 2L^2 & 0 & 0 \\ -12L & -6L & 24 & 0 & -12 & 6L \\ -6L^2 & -4L^2 & 0 & 8L^2 & -6L & 2L^2 \\ 0 & 0 & -12 & -6L & 12 & -6L \\ 0 & 0 & 6L & 2L^2 & -6L & 4L^2 \end{pmatrix} \begin{bmatrix} v_1 \\ \theta_1 \\ v_2 \\ \theta_2 \\ v_3 \\ \theta_3 \end{bmatrix} = \begin{bmatrix} P_{1y} \\ M_1 \\ P_{2y} \\ M_2 \\ P_{3y} \\ M_3 \end{bmatrix}$$

Boundary conditions for beam $v_1 = v_3 = \theta_1 = \theta_3 = 0$ (refer figure 8)

Where, P stands for the force and M stands for moment.

Reduced finite element equations,

$$\frac{EI}{L^3} \begin{Bmatrix} 24 & 0 \\ 0 & 8L^2 \end{Bmatrix} \begin{Bmatrix} v_2 \\ \theta_2 \end{Bmatrix} = \begin{Bmatrix} P_{2y} \\ M \end{Bmatrix}$$

For free vibration the force applied and the moments are zeros

$$\frac{\rho AL}{420} \begin{bmatrix} 312 & 0 \\ 0 & 4L^2 \end{bmatrix} \begin{Bmatrix} \ddot{v}_2 \\ \ddot{\theta}_2 \end{Bmatrix} + \frac{EI_z}{L^3} \begin{bmatrix} 24 & 0 \\ 0 & 8L^2 \end{bmatrix} \begin{Bmatrix} v_2 \\ \theta_2 \end{Bmatrix} = \begin{Bmatrix} 0 \\ 0 \end{Bmatrix}$$

Where, $\rho AL = m$ the total mass of the beam and rearrnging,

$$\begin{bmatrix} 312 & 0 \\ 0 & 4L^2 \end{bmatrix} \begin{Bmatrix} \ddot{v}_2 \\ \ddot{\theta}_2 \end{Bmatrix} + \frac{420EI_z}{mL^3} \begin{bmatrix} 24 & 0 \\ 0 & 8L^2 \end{bmatrix} \begin{Bmatrix} v_2 \\ \theta_2 \end{Bmatrix} = \begin{Bmatrix} 0 \\ 0 \end{Bmatrix}$$

The eigen value equations are;

$$[K - \omega^2 M] \phi = 0 \dots\dots\dots 3.6$$

$$[K - \lambda M] \phi = 0 \dots\dots\dots 3.7$$

$$\det[K - \lambda M] = [K - \lambda M] = 0 \dots\dots\dots 3.8$$

By solving the equation 3.6 and 3.7 we can get a polynomial of λ of order N this equation will have N roots $\lambda_1, \lambda_2, \dots \dots \dots \lambda_N$ Called eigen values, which relate the natural frequency of the system.

$$\text{Let, } X = \frac{420EI_z}{mL^3},$$

$$\det \begin{bmatrix} 24X - \lambda 312 & 0 \\ 0 & 8XL^2 - 8\lambda L^2 \end{bmatrix} = 0;$$

Solution;

From rail way transportation datas [1];

Where; $L=30\text{m}$

$$EI=130\text{NM}^2$$

$$X = 420EI / mL^3 = 332.88$$

$$(24X - \lambda^3)(8XL^2 - 8\lambda L^2) = 0$$

$$332.8 - 13\lambda - \lambda^2 = 0$$

Therefore using quadratic equation;

$$\lambda_1 = \frac{12.865 \text{ rad}}{\text{sec}}, \text{ and } \lambda_2 = \frac{-25.865 \text{ rad}}{\text{sec}}, \text{ since } \omega = \lambda^2$$

To have non trivial or non zero solution for \emptyset .

$$\omega_1 = \frac{165.5 \text{ rad}}{\text{sec}}, \omega_2 = \frac{669 \text{ rad}}{\text{sec}} \dots; \omega_1 = 4.19 \text{ Hz. and } \omega_2 = 106.5 \text{ Hz.}$$

From this we can say that, the catenary system should not to operate at 4.19Hz and 106.5Hz and for the speeds we select earlier is safe from resonance occurrence in the system.

3.4. Developing the contact point between the pantograph-catenary system

3.4.1. Theory of contact stress(Hertzian contact stresses)

The first successful analysis of contact stresses is attributed to Hertz [16]. This analysis gave the dimensions of the contact area and the pressure distribution over that area. These quantities permit the computation of the displacements and stresses in the neighborhood of the region of contact.

Assumptions for Hertzian Contact Theory

- Adhesion is neglected. Contacting bodies can be separated without adhesion forces (friction is neglected).
- Surfaces are continuous and non-conforming, i.e. the initial contact is a point or a line.
- Pressures within the materials are small enough to cause only elastic deformations.

- The area of contact is much smaller than the characteristic radius of the body.
- The surfaces are perfectly smooth, i.e. only a normal force acts between the parts in contact.

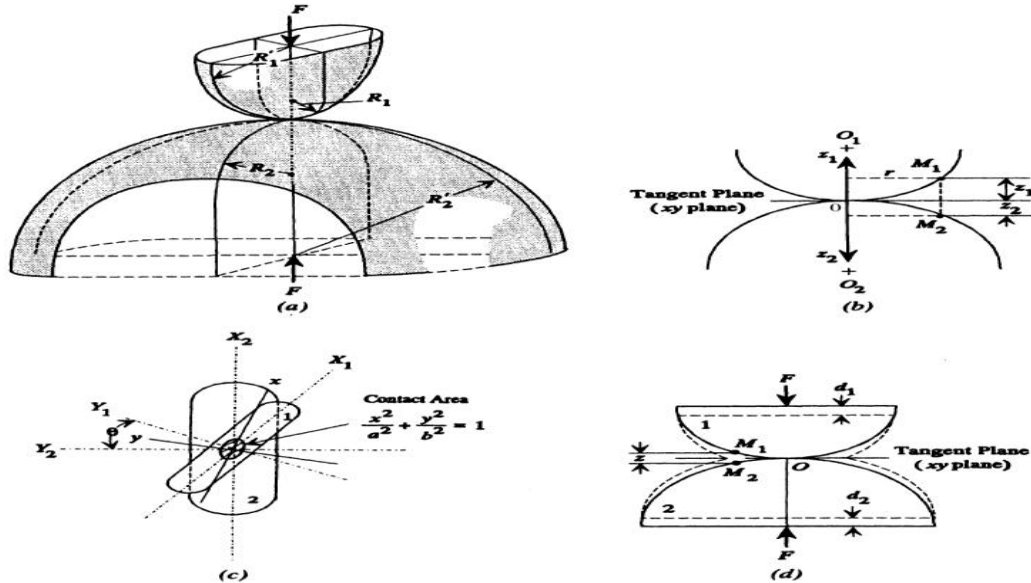


Figure 9: Two elastic solids in contact,(a)contact configuration; (b) before loading; c) after loading xy axis coincides with major and minor axis of elliptical contact area (hatched area), (d) Displacement of the contacting point M1 and M2 and rigid distance of approach $d=d_1+d_2$ [16]

Hoersch [22] performed important calculations of the stress fields in contacting solids.

The curvature of a surface is characterized at any point by the maximum and minimum values of the radii of curvature R' and R . The two planes are orthogonal and contain R' and R and the surface normal. A radius of curvature of the surface of a body is taken to be positive at a point if the corresponding center of curvature lies within the solid body; otherwise, the radius is negative. The coordinate system $(x, y, \text{ and } z)$ is aligned such that the xy plane lays tangent to the undeformed surfaces at the initial point of contact and such that the z axis coincides with the line of action of the force. Before deformation, suppose that the surfaces of the two bodies are approximately quadratic near the point of contact:

$$z_1 = A_1x^2 + B_1y^2 + C_1xy \dots\dots\dots 3.9$$

$$z_2 = A_2x^2 + B_2y^2 + C_2xy \dots\dots\dots 3.10$$

Where z_1 and z_2 are the perpendicular distances from the tangent plane to any point on the surfaces of body 1 and body 2 near the point of contact, respectively, in the z direction (Fig...9d) After deformation, two points that come into contact will have moved a distance.

$$z_1 + z_2 = (A_1 + A_2)x^2 + (B_1 + B_2)y^2 + (c_1 + c_2)xy \dots \dots \dots 3.11$$

The constants A and B are functions of the four principal radii of curvature of the two undeformed surfaces and of the orientation of the principal planes of curvature of body 1 with respect to those of body 2 (Fig...7):

$$A = 1/4 \left(\frac{1}{R_1} + \frac{1}{R_2} + \frac{1}{R_1^l} + \frac{1}{R_2^l} \right) - \frac{1}{4} \left\{ \left[\left(\frac{1}{R_1} - \frac{1}{R_1^l} \right) + \left(\frac{1}{R_2} - \frac{1}{R_2^l} \right) \right]^2 - \left[4 \left(\frac{1}{R_1} - \frac{1}{R_1^l} \right) \left(\frac{1}{R_2} - \frac{1}{R_2^l} \right) \sin^2 \theta \right] \right\} \dots \dots \dots 3.12$$

$$B = 1/4 \left(\frac{1}{R_1} + \frac{1}{R_2} + \frac{1}{R_1^l} + \frac{1}{R_2^l} \right) + \frac{1}{4} \left\{ \left[\left(\frac{1}{R_1} - \frac{1}{R_1^l} \right) + \left(\frac{1}{R_2} - \frac{1}{R_2^l} \right) \right]^2 - \left[4 \left(\frac{1}{R_1} - \frac{1}{R_1^l} \right) \left(\frac{1}{R_2} - \frac{1}{R_2^l} \right) \cos^2 \theta \right] \right\} \dots \dots \dots 3.13$$

To find the total displacement caused by the pressure p over the contact area, the elemental displacements are superimposed by integrating over the contact area A_c as shown in Eq. (3.11).

Hertz found that Eq. 3.11) is satisfied if $\mathbf{p}'(\mathbf{x}, \mathbf{y})$ is given by

$$p'(x, y) = p'_o \sqrt{1 - \left(\frac{x^2}{a^2} \right) - \left(\frac{y^2}{b^2} \right)} \dots \dots \dots 3.14$$

In which a , is the semi major axis and b the semi minor axis of the contact ellipse. The distribution of pressure is semi ellipsoidal with a maximum pressure p'_o at the center of the contact area and P_o the contact force between pantograph-catenary.

$$p'_o = 3P_o / 2\pi ab \dots \dots \dots 3.15$$

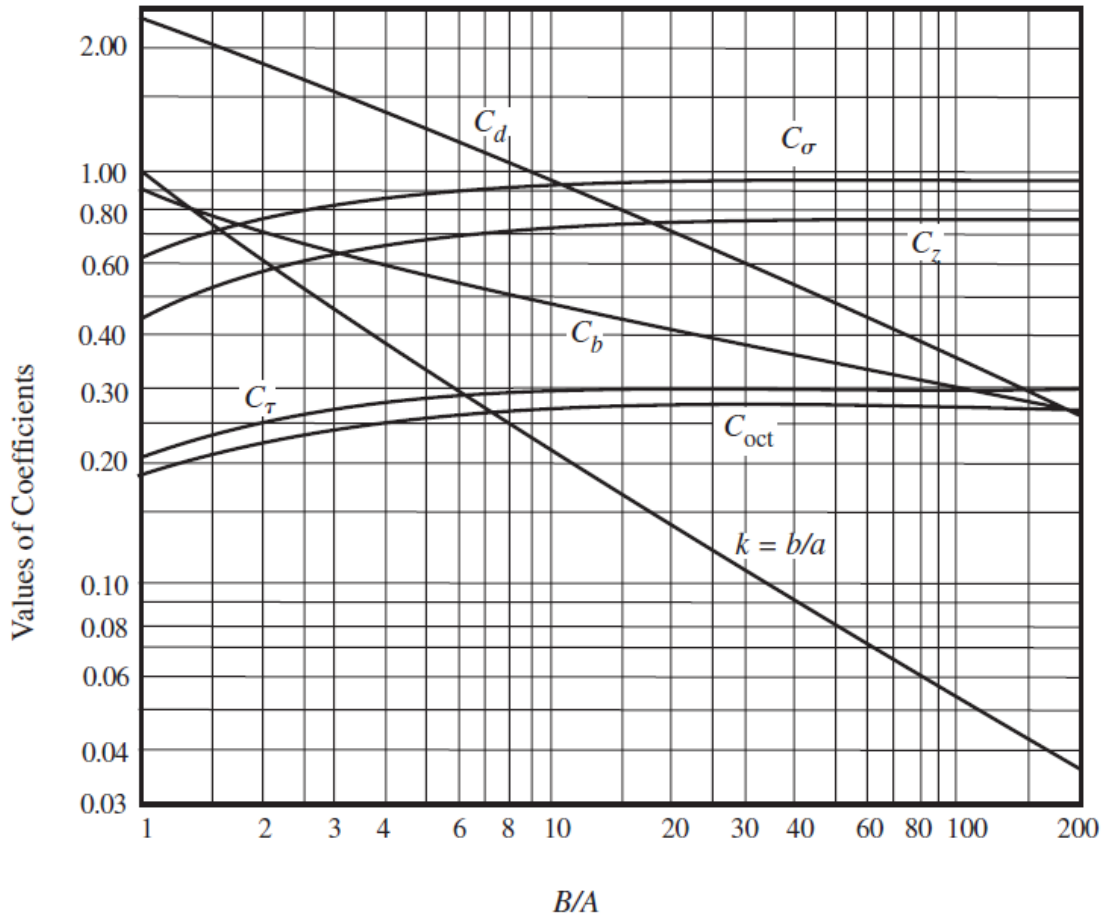


Table 8 : Coefficients for bodies in contact[2]

$$b = C_b(P\Delta)^{1/3} \dots\dots\dots 3.16$$

Where, $\Delta = \left(\frac{1-\nu^2}{E_1} + \frac{1-\nu^2}{E_2} \right) \frac{1}{A+B} = \gamma \frac{1}{A+B}$;

$$\gamma = \frac{1-\nu^2}{E_1} + \frac{1-\nu^2}{E_2} \dots\dots\dots 3.17$$

Defining, the quantity k the ratio of the minimum to the maximum axis of the ellipse.

$$k = \frac{b}{a} \dots\dots\dots 3.18$$

The displacement d can be found by using the quantity C_d:

$$d = C_d \left(\frac{P}{\pi} \right) (A + B) / \left(\frac{b}{\Delta} \right) \dots\dots\dots 3.19$$

From Knowledge of the dimensions of the contact area and the pressure distribution over it, Thomas and Hoersch[23] derived the expression for the principal stresses along the z axis with in the contacting solids. For values of B/A, from the table 8, we can get the maximum compressive stress δ_c that occurs at the origin, The maximum shear stress τ_{max} occurs with in the bodies, The distance Z_s from the contact area at which at which the maximum shear stress occur[11].

$$\delta_c = (\delta_c)_{max} = -C_\sigma \left(\frac{b}{\Delta} \right) \dots \dots \dots 3.20$$

$$\tau_{max} = C_\tau \left(\frac{b}{\Delta} \right) \dots \dots \dots 3.21$$

$$Z_s = C_z b \dots \dots \dots 3.22$$

3.5. Analysis for the contact of catenary-pantograph

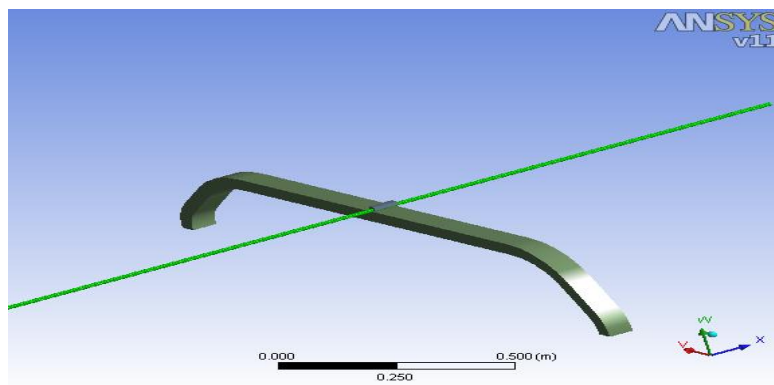


Figure 10: Modeling of contact wire-pantograph

Taken parameters are;

- $R_1 = \frac{12mm}{2} = 6mm, R_1' = \infty$ and $R_2 = 636mm, R_2' = \infty$
- The angle between the principal planes of pantograph-catenary is 90°
- The contact area assumed is an ellipse.

Therefore, $A=0.0007856; B=0.08333$; from equation... 3.12 and 3.13

$B/A=106.074$; and we can get the results from table...8;

$$c_{\tau} = 0.3$$

$$c_b = 0.3$$

$$c_{\delta} = 0.95$$

$$c_d = 0.37$$

$$k = 0.05$$

$$c_z = 0.76$$

We can get the major and minor axis of the ellipse contact area;

$b = C_b(P\Delta)^{1/3}$; where P is the uplift contact force in the pantograph-catenary system at speed of 70km/hr.

$$\Delta = 1.4035 * 10^{-10}; C_b = 0.3; P = 74.75N$$

$$b = 0.0006567m = 0.6567mm$$

The semimajor axis $a = \frac{b}{k} = 0.013134m = 13.134mm$;

Area of ellipse is ;

$$\pi a \times b = 3.14 \times 13.134 \times 0.6567 = 27.096543mm^2$$

- ❖ The compressive stress at the center of the contact ellipse (i.e., the maximum principal stress) becomes;

$$\delta_c = (\delta_c)_{\max} = -C_{\sigma} \left(\frac{b}{\Delta} \right) = -0.95(0.0006567/1.4035 * 10^{-10}) = 4.445Mpa = -7.786287Mpa$$

- ❖ The maximum shear stress

$$\tau_{\max} = C_{\tau} \left(\frac{b}{\Delta} \right) = 0.3(0.0006567/1.4035 * 10^{-10}) = 1403705.025pa = 1.4037Mpa$$

- ❖ The distance below the center of the contact area at which the two maximum shear stresses occur is found to be

$$Z_s = C_z b = 0.76(0.0006567) = 0.000499m = 0.499mm$$

3.6. In case of non- hertzian contact

The pantograph-catenary contact is subjected to sliding friction and it needs to consider the non hertzian contact.

3.6.1. Modeling of pantograph-catenary contact

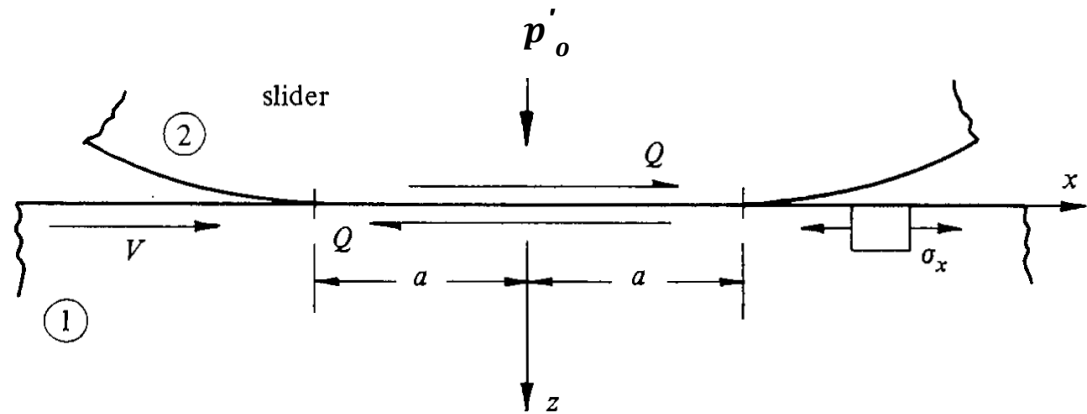


Figure 11: Modeling of pantograph-catenary wire while sliding

The maximum coefficient of friction subjected in the contact between pantograph-catenary system is 0.1. when it is more than that the contact between them will be disturbed[21]. The stress caused due to both pressure and frictional tractions are; [21]

$$\sigma_x = -p'_o \left\{ \left(1 - \frac{x^2}{a^2} \right)^{\frac{1}{2}} + 2\mu x/a \right\}$$

$$\sigma_z = -p'_o \left\{ \left(1 - \frac{x^2}{a^2} \right)^{\frac{1}{2}} \right\}$$

$$\sigma_y = -2\nu p'_o \left\{ \left(1 - \frac{x^2}{a^2} \right)^{\frac{1}{2}} + \mu x/a \right\}$$

Where,

a = the width of the contact area

p'_o = the pressure on contact point

ν = poissonse ratio.

μ = coefficient of friction

x = the contact point length in the direction of x-axis.

There fore;

$$p'_o = \frac{3P_o}{2\pi ab} = 4.13809245 \text{Mpa.}$$

at $x=0.01 \text{mm}$. $\sigma_x=3.7228 \text{Mpa}$. at $x=0.6567 \text{mm}$. $\sigma_x=0.748 \text{Mpa}$.

at $x=0.01 \text{mm}$ $\sigma_z=3.71 \text{Mpa}$. at $x=0.6567 \text{mm}$, $\sigma_z=0.0 \text{Mpa}$.

at $x=0.01 \text{mm}$, $\sigma_y=2.245 \text{Mpa}$, at $x=0.6567 \text{mm}$, $\sigma_y=0.2244 \text{Mpa}$.

The maximum stress occurs is $3.7228 \text{Mpa} < 300 \text{Mpa}$. (yield stress of copper wire [4])

Hence, we can say that considered dimensions and parameters are safe for operation based on contact mechanics analysis.

3.7. Fatigue life analysis

A catenary wire subjected to contact stresses usually fails after a large number of load applications. The failure mode is that of crack initiation followed by propagation until the part fractures or until pits are formed by material flaking away.

3.7.1. Analysis

- Contact wire has two major stresses
 - Tensile stress caused by tension
 - Bending stress caused by pantograph sliding
- Bending stress increases
 - with upward force of pantograph
 - with train running speed

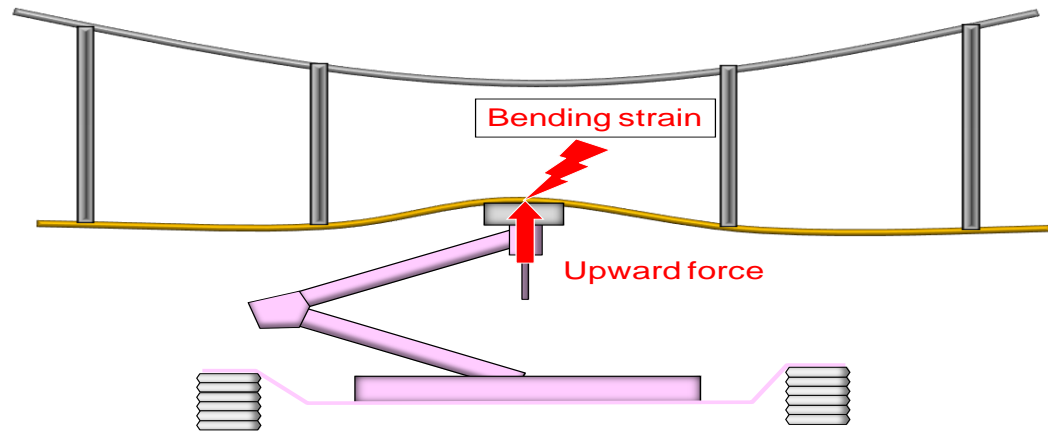


Figure 12: Pantograph-catenary interaction

If we use;

- High upward force of pantograph can lead to keep steady contact between the pantograph and OCL.
- Small upward force .
 - It can minimize breakdown of contact wire by fatigue from many passages of pantographs. However in case of high speed of the train, it needs to minimize contact loss.
 - So, it is necessary to maintain the contact of the pantograph and catenary system.

3.7.2. Trains technical specification based on international laws

N028: The IEP Trains must, at all speeds, accelerate at a rate no greater than that defined in the graph below, unless higher rates of acceleration are demonstrated to be compatible with the infrastructure: [22]

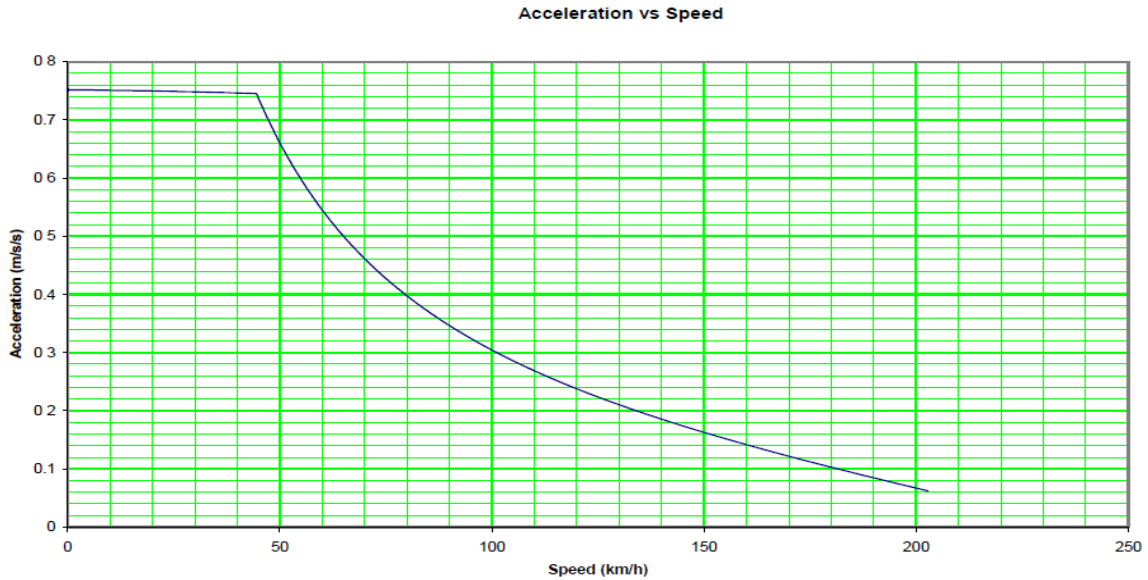


Table 9 : Technical specifications for relating acceleration vs speed

3.8. Displacement of the contact wire in the Y direction.

The uplift of the contact wire y_o at the contact point with the pantograph can be expressed as [6]:

$$y_o = \frac{P_o}{\sqrt{2\sqrt{k_o T} \sqrt{1-(v/c)^2}}} \dots\dots\dots 3.23$$

Where,

P_o is the lifting force of the pantograph when the train is at rest, K_o is the equivalent spring constant, v is the speed of the train. When $v \rightarrow c$, y_o becomes too large. Hence to make the current collection uninterrupted when speed increase, the wave propagation speed has to be increased, i.e., the tension T in the overhead contact wire has to be increased. This led to the development of improved contact wires like the TA or CS type, presently being used in Japan, where there is a steel reinforcement at the core of the overhead contact wire to make it capable of withstanding more tensile stress [7].

$P_o=12.5N$ [36], $V=70km/hr$.

$K_o=180000N/m$; $T=12000N$

$$y_0 = \frac{12.5}{\sqrt{2\sqrt{180000(12000)}\sqrt{1-(70/398.18)^2}}} = 0.04164 = 41.65\text{mm}$$

3.9. Modeling the catenary wire by using ANSYS soft ware



Figure 13: The photo shows the tensioning system of contact wire [12]

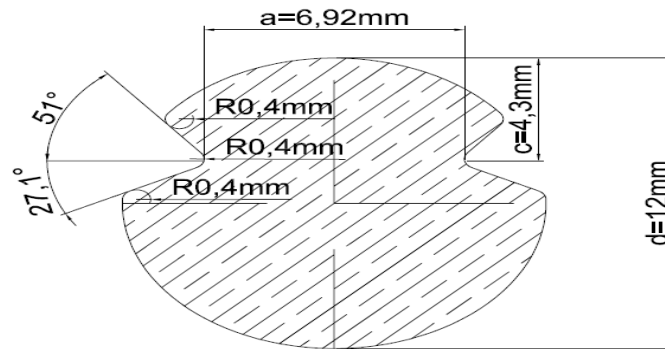


Figure 14: Front view of contact wire and its standard dimension

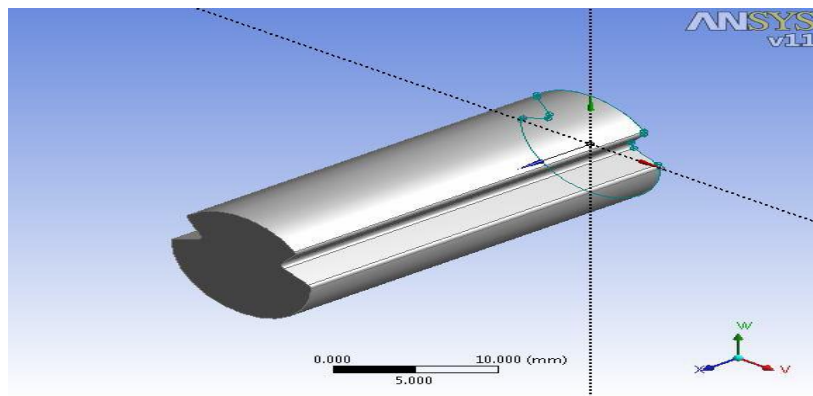


Figure 15: Contact wire modeled via ANSYS soft ware

- The recorded data show that, most fatigue failure occur on Junction claw as shown below.[10]



Figure 16: Junction claw photos [9]

- Considering the junction claw as undeformed object. Thus, we can model via Ansys software as in fig....13)



Figure 17: Dropper clamped onto the contact wire (Photo: Petter RøeNåvik). [8]

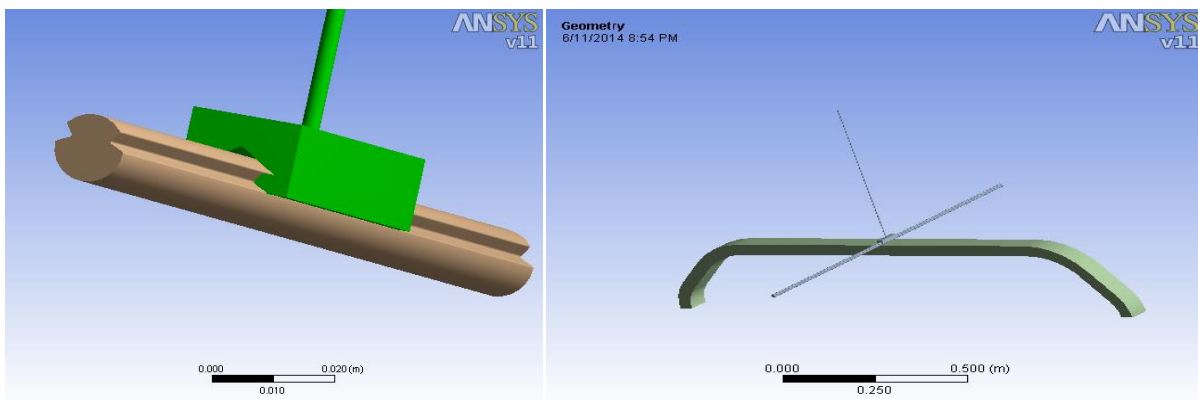


Figure 18: Modeling of contact wire with junction claw via ANSYS software

3.9.1. Meshing

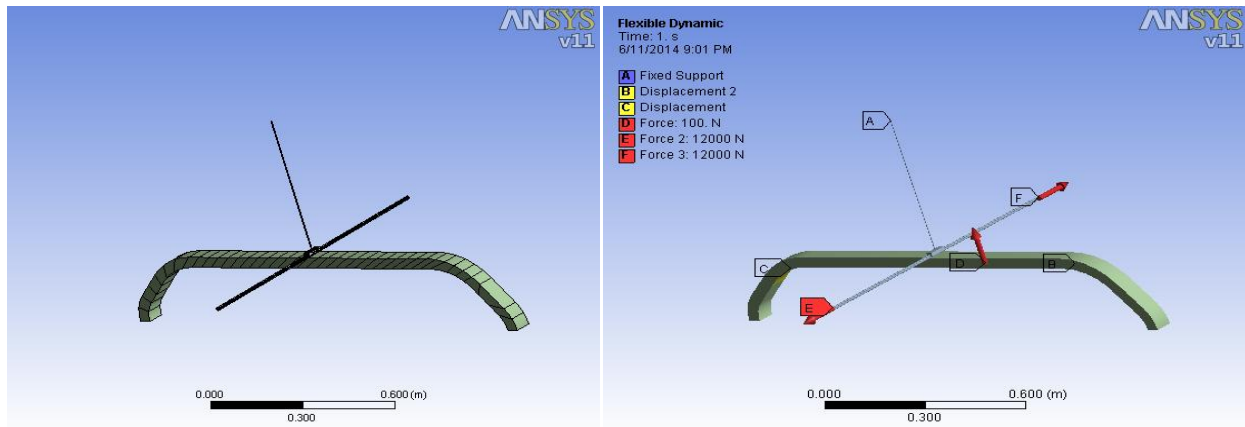


Figure 19: a) Meshing of catenary system (left) b) Force analysis of catenary system (right)

CHAPTER FOUR

SIMULATION RESULTS AND DISCUSSION

4.1. Predicting Fatigue life of the catenary wire via ANSYS soft ware

This result contour plot shows the available life for the given fatigue analysis. If loading is of constant amplitude, this represents the number of cycles until the part will fail due to fatigue. If loading is non-constant, this represents the number of loading blocks until failure. Thus if the given load history represents one month of loading and the life was found to be 120, the expected model life would be 120 months.

In a constant amplitude analysis, if the alternating stress is lower than the lowest alternating stress defined in the S-N curve, the life at that point will be used. (Taken from ANSYS help)

The ansys results in the figure 19 indicate that the contact wire has the maximum fatigue life 1×10^6 cycles and the smallest fatigue life is 384.82 cycles when the pantograph is away from droppers the fatigue failure is at the top of the contact wire. When the pantograph is in the dropper as shown in the figure 20, the maximum fatigue life is 1×10^6 cycles and the smallest fatigue life is 63300 cycles. The part which fails due to fatigue is at the bottom side of the contact wire and near the Junction claw. This comparison indicates that the contact wire near the dropper has larger fatigue life than away from the dropper.

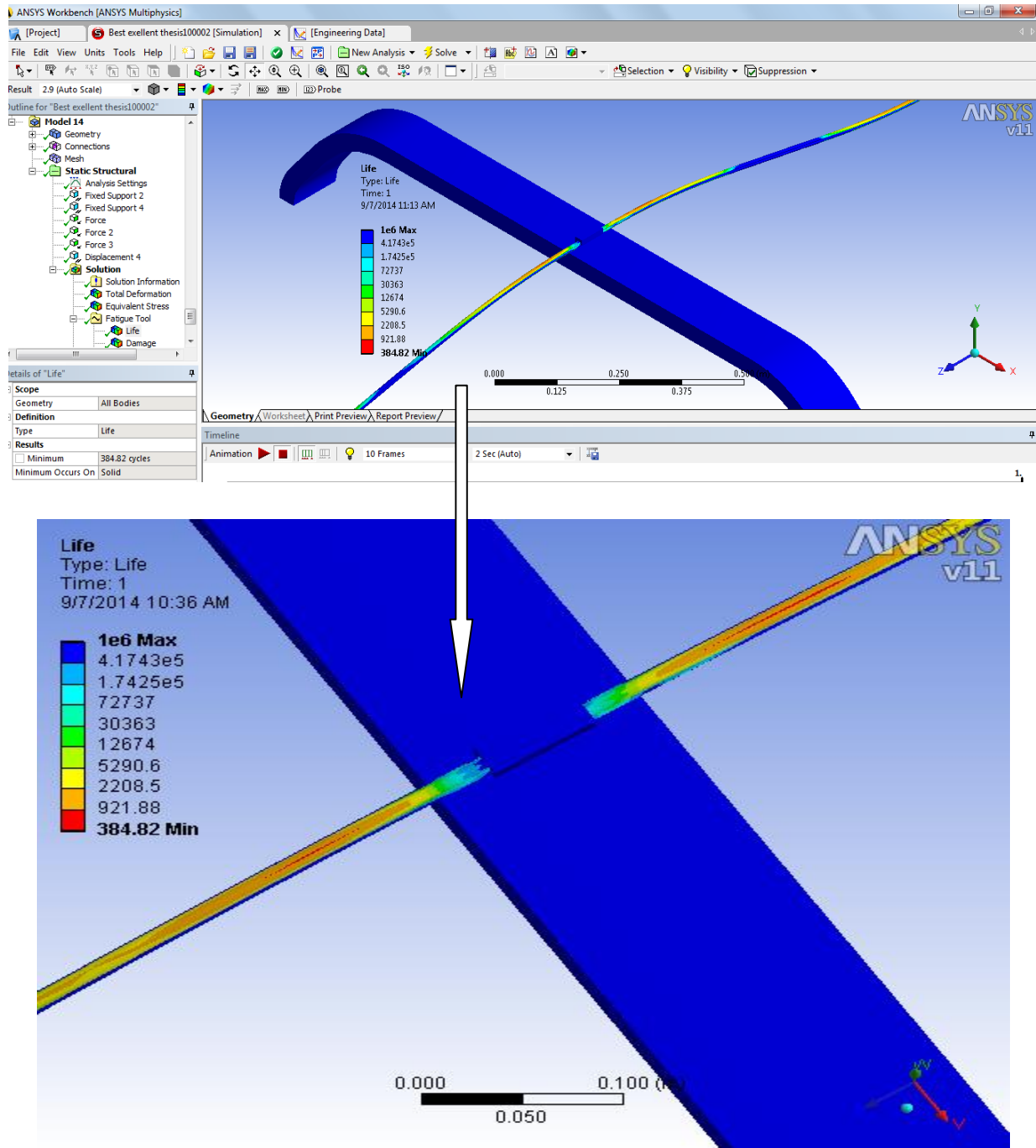


Figure 20: Fatigue life of the catenary system far from the droppers

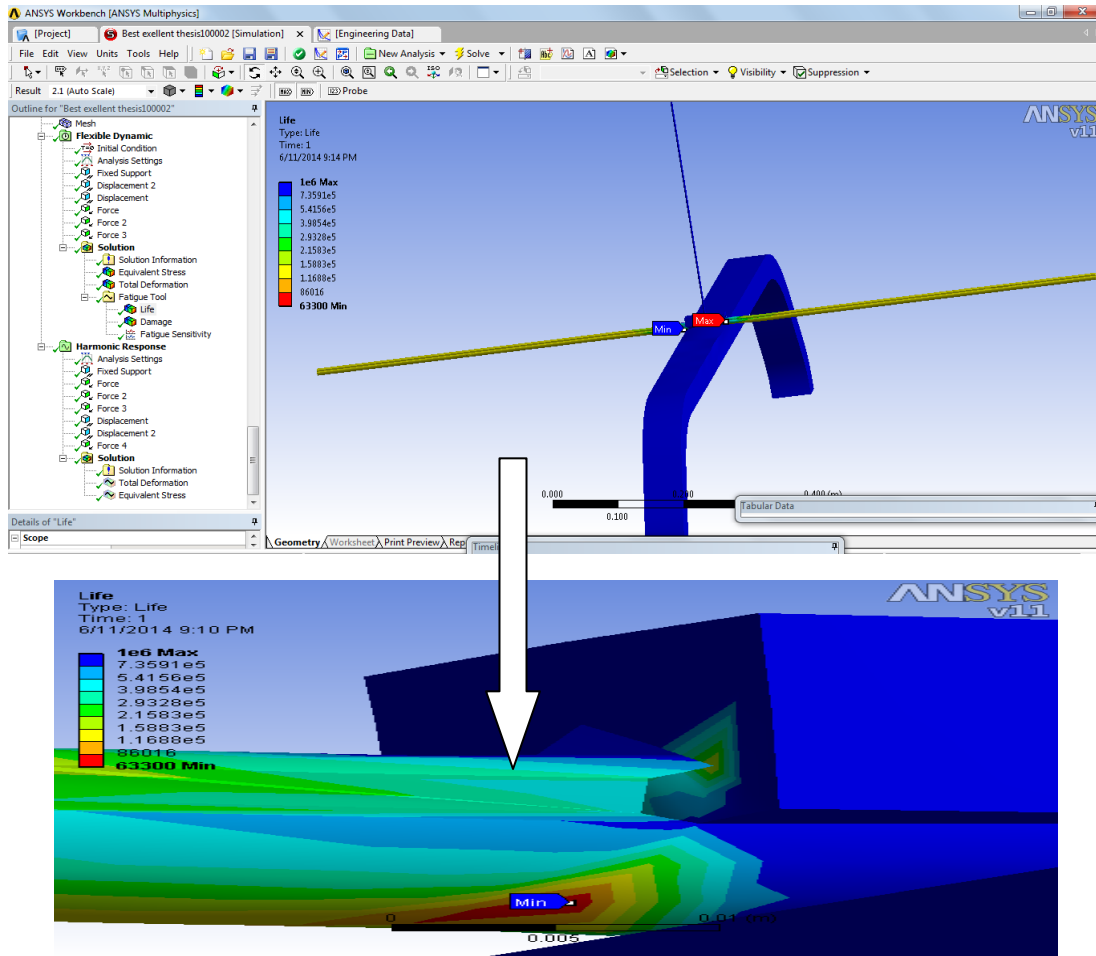


Figure 21: Fatigue life of the catenary system near o the droppers

- ❖ As we can see in the figure21 that the weakest fatigue life of the contact wire is at the bottom side of the contact between the pantograph and contact wire, near to the junction claw with a dropper. The contact wire is expected to fail at the bottom side of the contact due to cyclic load.

4.1.1. Von- misses Stress distribution in the catenary system with droppers and with out

Equivalent stress is related to the principal stress by the equation:

$$\delta_e = \left[\frac{(\delta_1 - \delta_2)^2 + (\delta_2 - \delta_3)^2 + (\delta_3 - \delta_1)^2}{2} \right]^{1/2}$$

Equivalent stress also called von Mises is often used in design work because it allows any arbitrary three-dimensional stress state to be represented as a single positive stress value. Equivalent stress is part of the maximum equivalent stress failure theory used to predict yielding in a ductile material. (Ansys help)

Stress Life always needs to query an SN curve to relate the fatigue life to the stress. By using alternating stress and fatigue life, it is possible to draw SN graph of the contact wire.

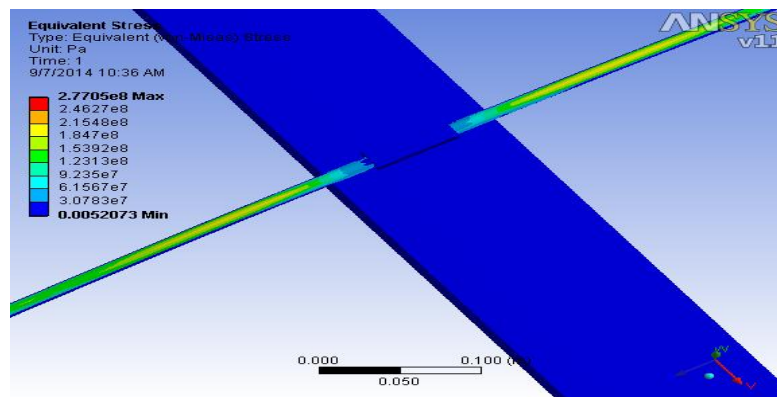


Figure 22: Equivalent stress pantograph-catenary system away from the dropper.

- ❖ The S-N curve shown (figure 21) that as the number of running cycle increases the contact wire yield stress will decrease and eventually the system will fail due to cyclic load (fatigue).

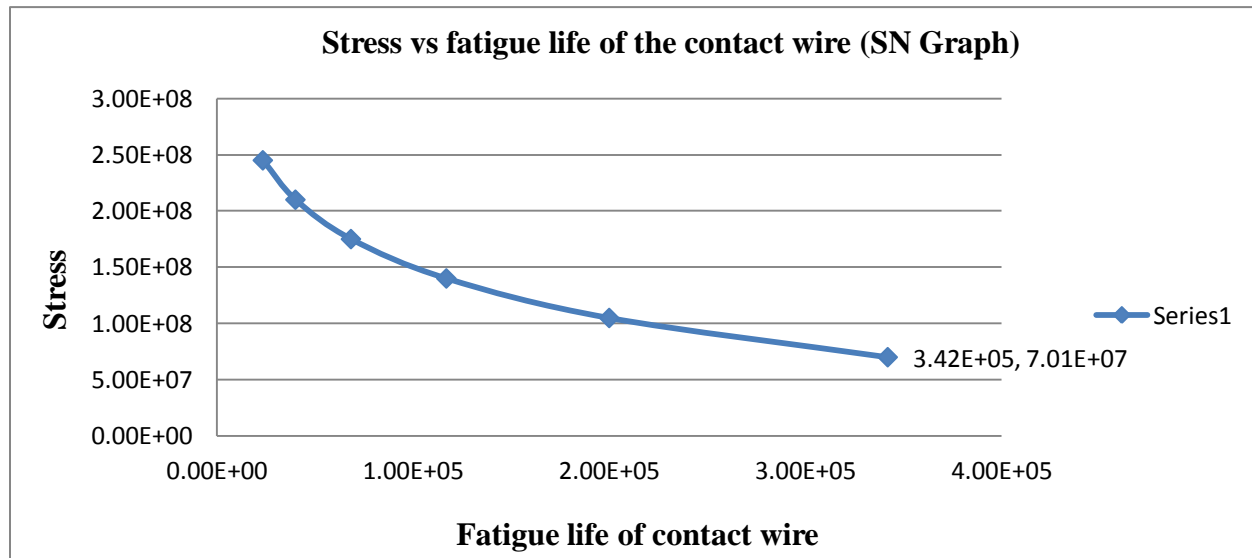


Figure 23: Stress vs cycle to failure of contact wire fatigue test analysis by ANSYS soft ware

4.1.2. Fatigue Sensitivity

This plot shows how the fatigue results change as a function of the loading at the critical location on the scoped region. Sensitivity may be found for life, damage, or factor of safety. For instance, if you set the lower and upper fatigue sensitivity limits to 50% and 150% respectively, and your scale factor to 3, this result will plot the data points along a scale ranging from 1.5 to 4.5 scale factor. You can specify the number of fill points in the curve, as well as choose from several chart viewing options (such as linear or log-log).

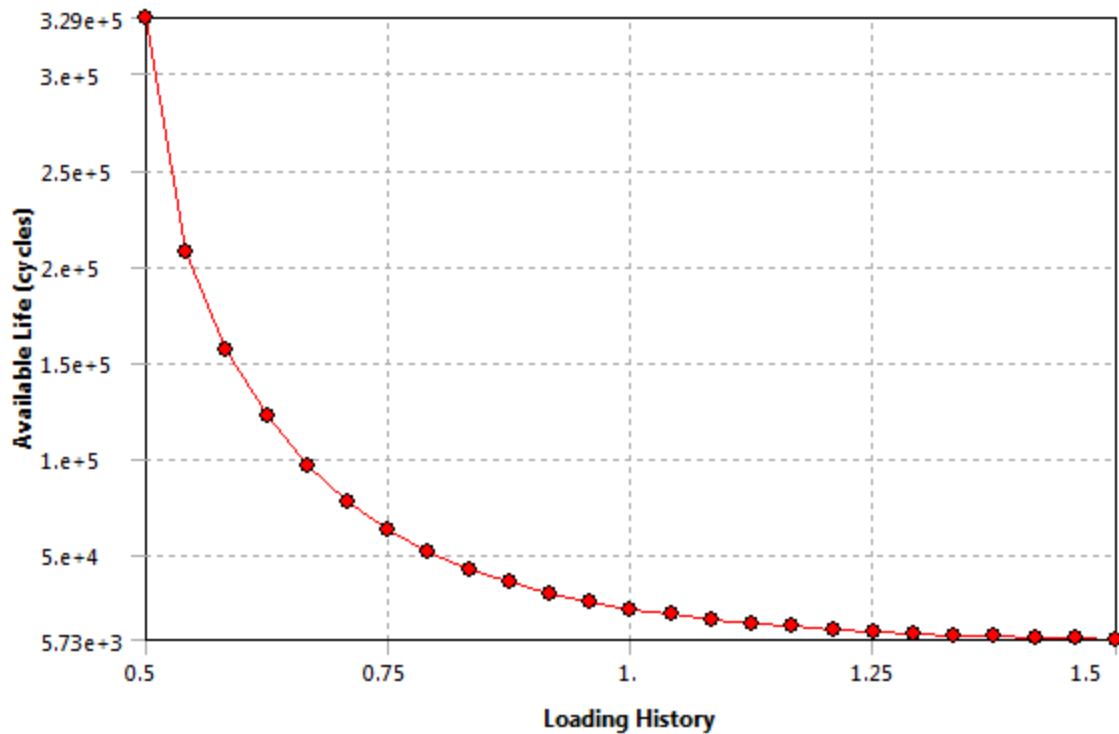


Table 10: Fatigue sensitivity of contact wire by ANSYS soft ware

From the above figure we can see that how the fatigue life change at 50% fatigue sensitivity, the available fatigue life is $3.29e+5$ cycles and when the fatigue sensitivity is 150% the remaining fatigue life is $5.73e+3$ cycles.

4.1.3. Hysteresis

In a strain-life fatigue analysis, although the finite element response may be linear, the local elastic/plastic response may not be linear. The Neuber correction is used to determine the local elastic/plastic response given a linear elastic input. Repeated loading will form close hysteresis loops as a result of this nonlinear local response. In a constant amplitude analysis a single hysteresis loop is created although numerous loops may be created via rain flow counting in a non-constant amplitude analysis. The **Hysteresis** result plots the local elastic-plastic response at the critical location of the scoped result (the **Hysteresis** result can be scoped, similar to all result items). **Hysteresis** is a good result to understand the true local response that may not be easy to infer. (ANSYS help)

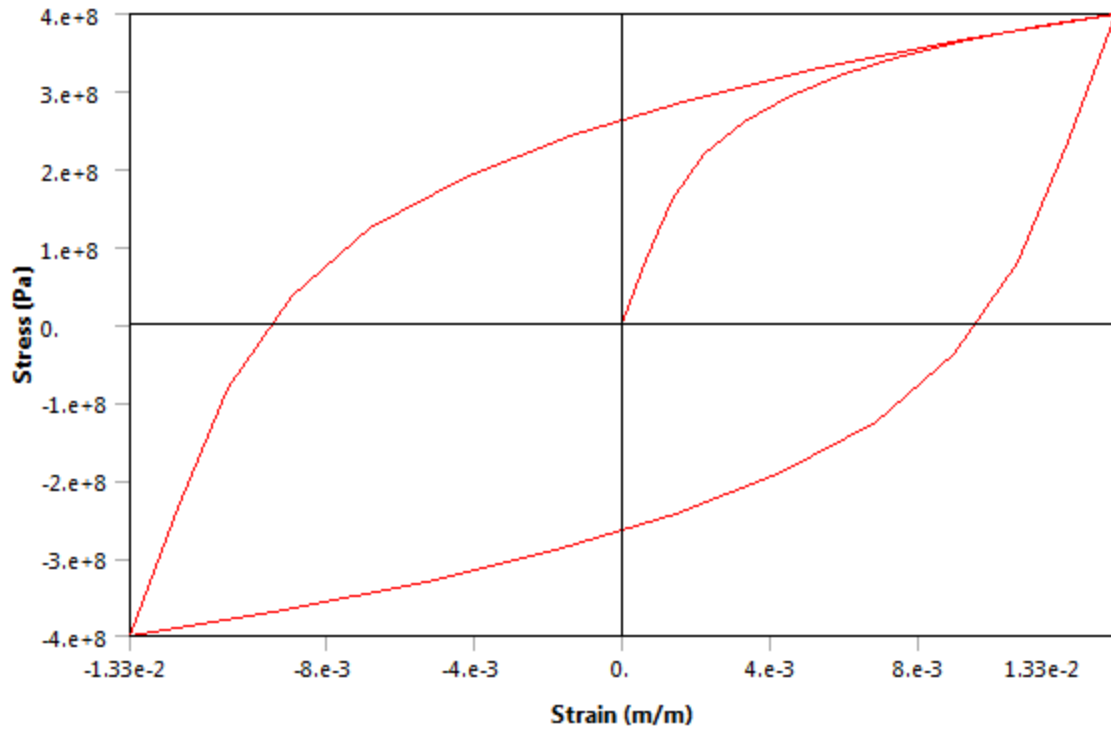


Table 11: Stress-strain graph of contact wire via ANSYS soft ware

4.1.4. Damage

Fatigue damage is defined as the design life divided by the available life. A damage of greater than 1 indicates the part will fail from fatigue before the design life is reached [34]

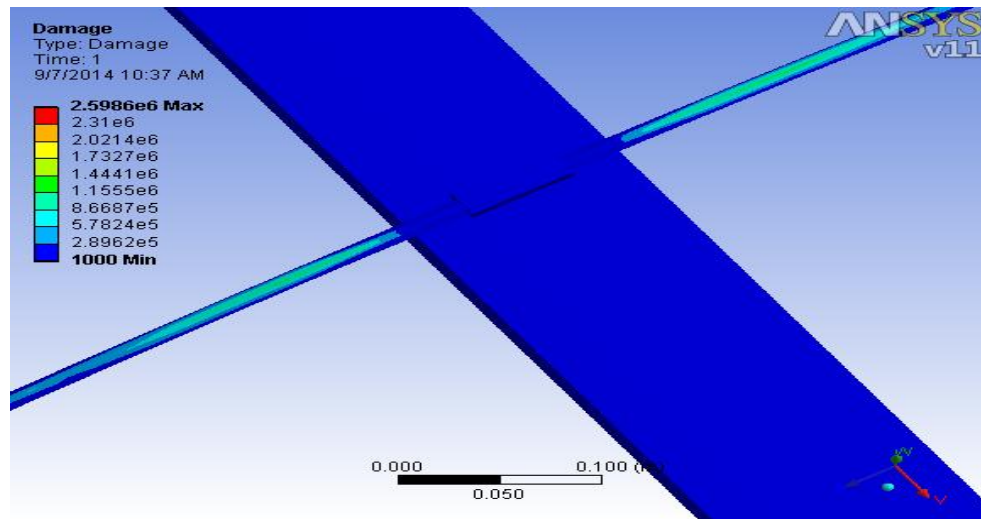


Figure 24: Fatigue damage of contact wire via ANSYS soft ware

The figure 24 indicates that the contact wire which damage early shown at the top side of the catenary wire , therefore preventive and proactive maintenance has to be applied, in order to in large the life of the catenary wire.

4.1.5. Fatigue Factor of Safety at a Design Life

Fatigue factor of safety Contour plot of the factor of safety with respect to a fatigue failure at a given design life. Maximum Factor of Safety displayed is 15, like damage and life, this result may be scoped. For Fatigue Safety Factor, values less than one indicate failure before the design life has been reached [34].

Figure 24 indicates that at the bottom and top side of the contact wire the fatigue sensitivity is less than one, and this indicates that the contact wire is expected to fail at those positions due to cyclic load (fatigue) before the designed life. Hence, it is possible to predict that the contact wire is expected to fail earlier than designed life.

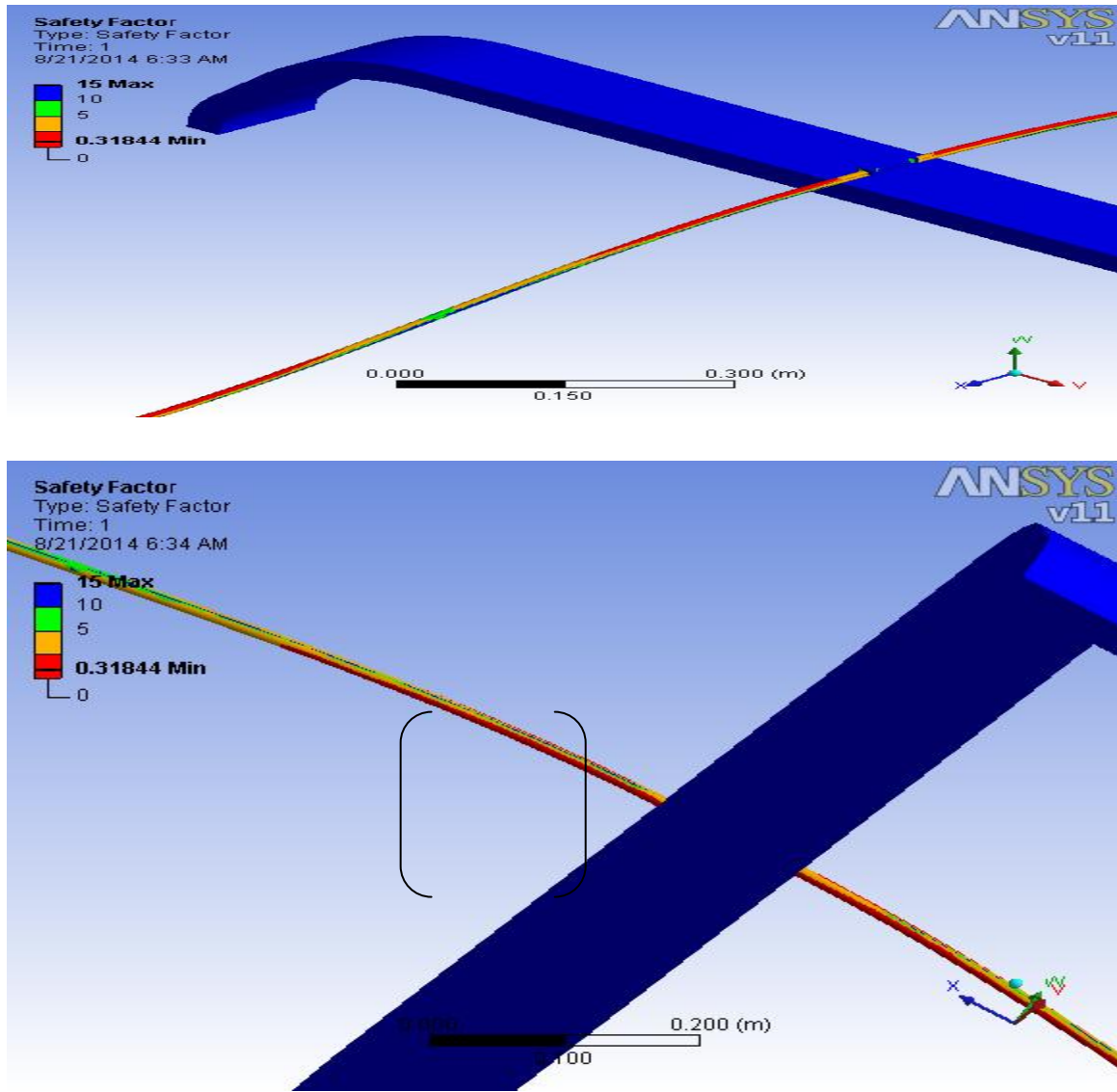


Figure 25: Safety factor of pantograph-catenary system

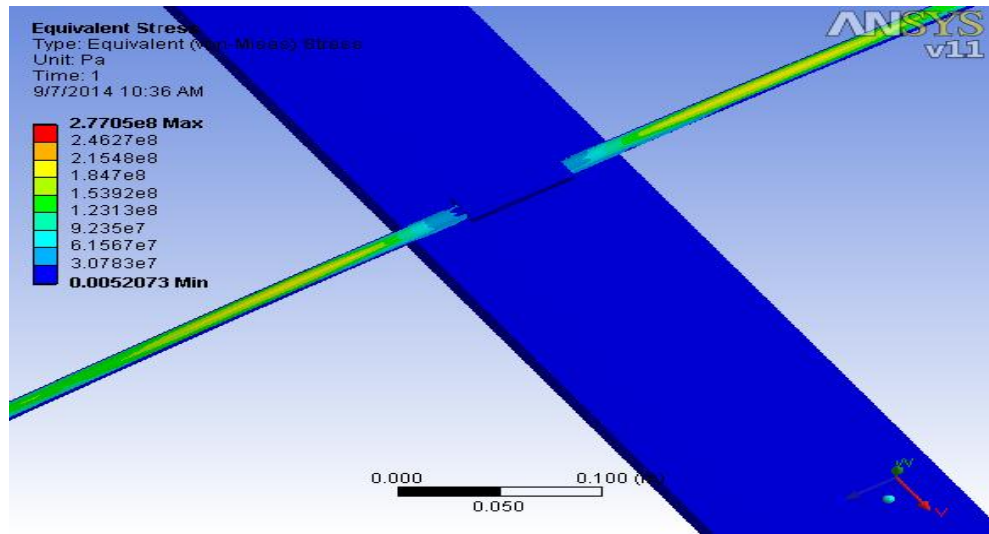


Figure 26: Static Vonmises stress of contact wire far from the droppers

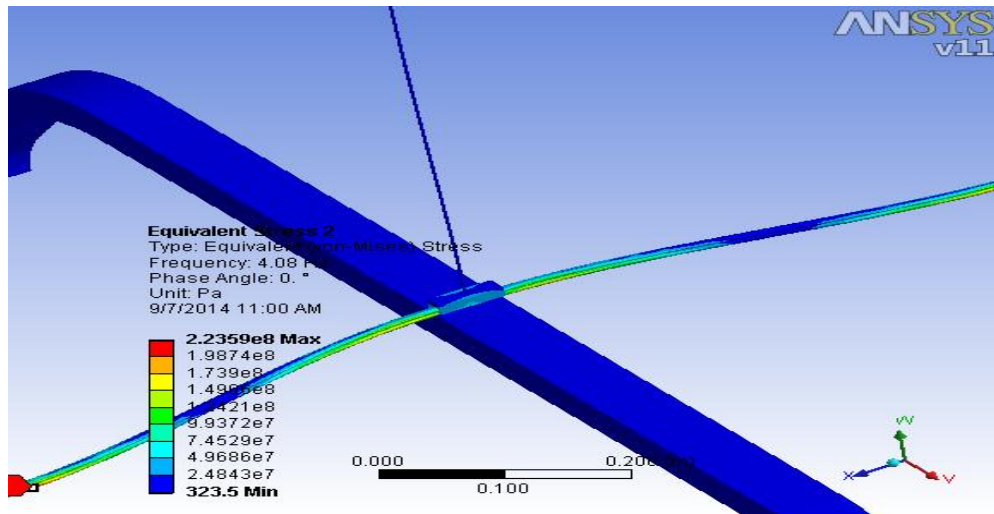


Figure 27: Dynamic Vonmises stress of contact wire near to the droppers

4.2. Comparing results of contact wire with droppers and with out

- In case of contact wire droppers there occurs more stress on the junction claw than without. This leads to early failure to fatigue stress and damage to the contact wire.

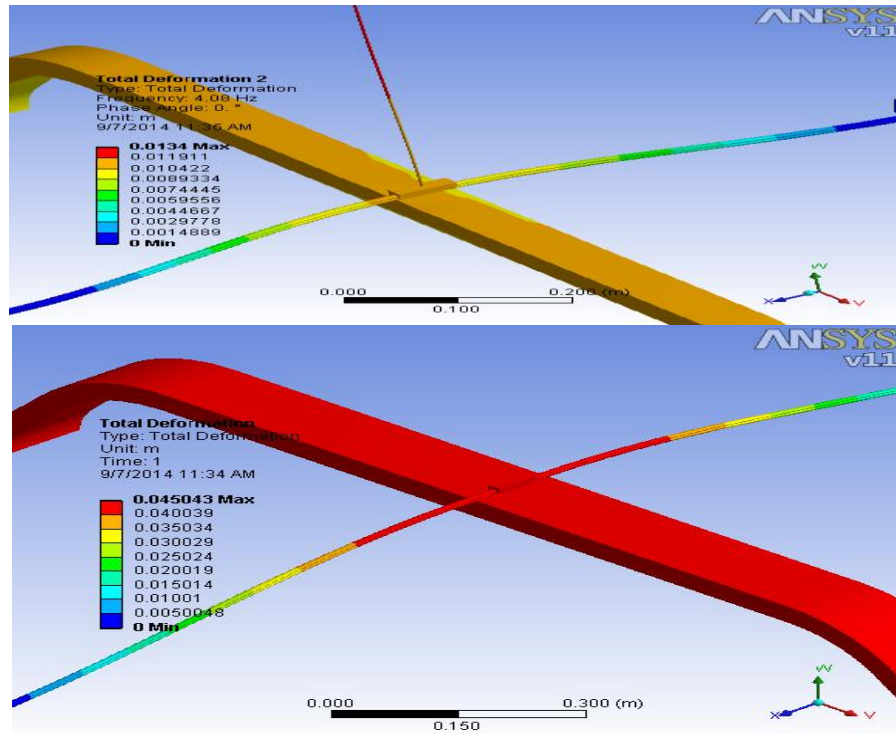


Figure 28: Total deformation of the contact wire in areas of droppers and far from droppers

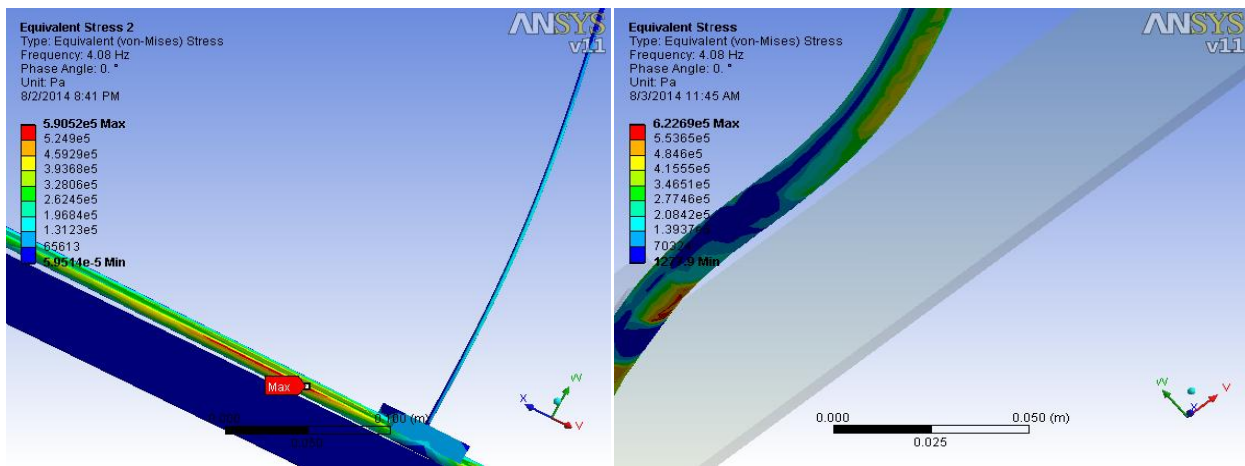


Figure 29: Dynamic Vonmises stress of contact wire with and without droppers

In the figure 27 we can observe that having dropper wires the Vonmises stress of the contact wire is 5.9052×10^5 pa. and without droppers the Vonmises stress is 6.2269×10^5 pa. this

indicates that, having the droppers decreases the occurrence of early failure of contact wire due to fatigue wear.

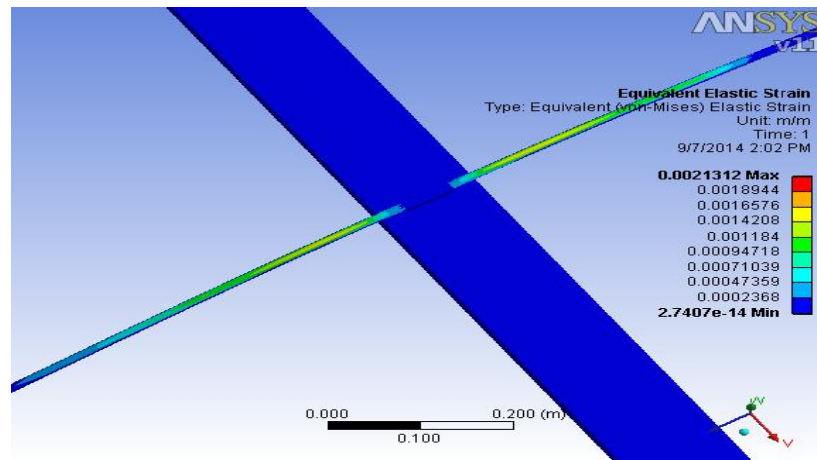


Figure 30: The maximum shear elastic strain of pantograph-catenary system

4.3. Catenary-Pantograph interaction model

The dynamic performance of the catenary-pantograph system has been validated in accordance with the European standard EN50318 [22]. This standard establishes the requirements for the validation of a catenary-pantograph interaction computational model. Essentially, this norm establishes a benchmark theoretical catenary-pantograph system and the range of results that must be accurately predicted by a simulation code.

Maximum uplift at different position is

- Maximum uplift range is = 55-65mm [22]

The maximum uplift of the contact wire calculated in this thesis work via ansys soft ware is **13.4mm < 55mm near to droppers** and **45.04 mm < 55mm** far from the droppers, which is the maximum up lift of the contact wire based on European standard.

The maximum Vonmises stress 277.05 Mpa occurs away from the droppers and 223.59Mpa near to the droppers .Both conditions have less stress than yield stress of copper wire 300 Mpa [4].Thus, the conditions consider are safe for the operation of the catenary-pantograph system. We can analyze here that, if the number of the droppers are increased, it is possible to increase the life of the contact wire.

4.4. Summary

The overhead conductor system (OCS) could be one of the most economical and feasible engineering solutions to transmit electrical energy to intercity trains along open or tunnel routes. However, the consumption of contact wire and collector strips due to wear and tear could impose a severe cost on the railway so it is always desirable to have a model able to predict the contact wire and collector strip interaction performance for good current collection and to minimize wear and tear of both interacting materials. In this thesis it deals on the over head contact wire wear life which occurs due to cyclic load (fatigue) by analyzing using contact mechanics, ANSYS soft ware results and relating experimental results carried out by RTRI (fatigue life test on contact wire).In addition, it compares the fatigue life of the catenary systems near and far from droppers. The output of the results is the life of contact wire is week at the junction claw and it is similar with experimental results.

CHAPTER FIVE

CONCLUSION, RECOMMENDATION AND FUTURE WORK

5.1. CONCLUSION

The conclusion from this master thesis research is that the developed model of pantograph-catenary system able to predict the fatigue life of contact wire via ANSYS work bench soft ware. To address such objective the contact point is developed by using contact mechanics and analyze its deflection, stress distribution on the contact wire. And then, the catenary and pantograph contact point is analyzed using numerical analysis, modeled and predict its fatigue life of the contact wire through ANSYS soft ware. The result is compared and contrast with experimental results achieved by railway organization. From results one can see that, it is possible to predict the contact wire fatigue life and this can safe maintenance cost, disturbance in the operation of transportation and increase the profitability of the organization. Beside this the paper compares the effect of contact wire near to droppers and away from them, and observe that the fatigue life will increase when there is droppers. Thus, it is better to use more flexible droppers which has less compressive stress. Moreover, we can see that the weakest life of the contact wire is at the bottom of the contact wire near to the droppers and at the top of the contact wire far from the droppers. In the pre-tensioned beam, the wave propagation speed increases as the frequency increases. Thus, high frequency waves move faster than low-frequency waves [11]. And, we can see table 6 as speed increase, the frequency of the catenary system simultaneously increase.

The pantograph-catenary system is subjected to vibration while transmitting electrical energy to electrical motors at different speeds of the train. Hence, the contact wire will subject to resonance when the driving frequency and the natural frequency of the system are equal; this condition is destructive to the catenary system earlier than its fatigue life. Therefore, the research identifies the speeds that can cause resonance and the selected speeds are free from the occurrence of it.

In general, it is possible to predict the fatigue life of the contact wire, which happens without any warning, through ANSYS work bench soft ware. Hence, this thesis will be helpful for railway organizations and the country at large in enhancing the economy.

5.2. RECOMMENDATION

- In today's railway system high speed trains are introduced in the market, indeed they use multiple pantographs. So, it is better to consider fatigue life of contact wire for future work when using pantograph more than one.
- Here the effect of the vertical displacement is only considered, but the contact wire will be displaced in the lateral, longitudinal direction.
- The corrugations of the wheel and rail and defective suspension spring have a direct effect on the catenary-pantograph system. However, in this thesis work it is neglected for future work.
- From the results we can understand that, preventive maintenance has to be carried out in the junction claws and droppers holders.
- Rail way organizations should not to operate trains at speed, which could create resonance to the catenary system.

5.3. FUTURE WORK

The pantograph-catenary system is subjected to cyclic load (fatigue), while delivering electrical power to the motors. But, here the selected speed of the train is based on Ethiopian rail way corporation running speed standard for trains working in Addis Ababa city. Therefore, it is possible to consider for high speed trains as a future work. The corrugation of rails, suspension system, centrifugal forces of curves of rails have an effect on the contact wire fatigue system and it is left as a future work.

It is also possible to see the effect of fatigue by changing the material properties of the contact wire and the pantograph.

Many rail ways are now using multiple pantographs, and it is better to consider the effect of fatigue failure of the contact wire, and building laboratory model based on Ethiopian rail way corporation infrastructure is obviously suggested as well for future work.

REFERENCE

- [1] J.P. Massat¹, T.M.L. Nguyen-Tajan¹, H. Maitournam², E. Balmès³ and A. Bobillot “Fatigue analysis of catenary contact wires for high speed trains.” May 22-26, 2011
- [2] Arnar Kári Hallgrímsson “Dynamic behavior of contact lines for railways with laboratorial model setup according to Norwegian conditions.” Department of Structural Engineering, Norwegian University of Science and Technology, June 2013.
- [3] K.L. JONSON “Contact mechanics” Emeritus Professor of Engineering, University of Cambridge 2003.
- [4] Yongseok Kim¹, Li Haochuang¹, Chang-Sung Seok¹, Jae-Mean Koo¹, Kiwon Lee², Sam-Young Kwon² “Fatigue Life Prediction Method for Contact Wire Using Maximum Local Stress” 9th International Conference on Fracture & Strength of Solids June 9-13, 2013, Jeju, Korea
- [5] A. Bobillot, L.M. Cléon, A. Collina, O. Mohamed, R. Ghidorzi, “Pantograph-Catenary: a High-Speed European couple”. In: Proceedings of the World Congress on Railway Research, 2008.
- [6] Tiago Manuel Oliveira Valezim Teixeira “Dynamics and Control of a High Speed Train Pantograph System” September 2007
- [7] Yong Hyeon Cho “Influence of contact wire pre-sag on the dynamics of pantograph–railway catenary” 31 August 2009
- [8] T. Dahlberg, "Moving force on an axially loaded beam – with application to a railway overhead contact wire", *Vehicle System Dynamics*, 44 (8), 631-644, 2007
- [9] A. Sugahara, “Preventing Fatigue Breakage of Contact Wires”, *Railway Technology Avalanche* No. 24, September 19, 2008.
- [10] Yong Hyeon Cho “Numerical simulation of the dynamic responses of railway overhead contact lines to a moving pantograph, considering a nonlinear dropper” 18 April 2008

- [11] Surajit Midya “Conducted and Radiated Electromagnetic Interference in Modern electrified Railways with Emphasis on Pantograph Arcing.”KTH Electrical Engineering TRITA-EE 2009:029
- [12] Pedro Cabaço Antunes “Development of Multibody Pantograph and Finite Element Catenary Models for Application to High-speed Railway Operations.”october2012
- [13] Shing Wai Chung “A Survey of Contact Wire Wear Parameters and the Development of a Model to Predict Wire Wear by using the Artificial Neural Network.” September 2011.
- [14] E. Standard, Railway applications- Current collection systems - Technical criteria for the interaction between pantograph and overhead line (to achieve free access), Std. EN 50 367, 2006.
- [15] S. Kubo and H. Tsuchiya, Recent developments in the installation of carbon contact strips on pantograph heads," Quarterly Report of Railway Technical Research Institute, vol. 45, no. 4, Nov. 2004.
- [16] Hertz, H., Miscellaneous Papers, Macmillan, New York, 1896.
- [17] www.railwaypro.com “Railway infrastructure development for an efficient & green transport” February 23 – 24, 2011, Poiana Braşov
- [18] Simon Iwnicki “Hand book of railway vehicle dynamics” 2006.
- [19] A. Collina and S. Bruni, "Numerical Simulation of Pantograph-Overhead Equipment Interaction", Vehicle System Dynamics, 38 (4), 261-291, 2002
- [20] EN50318:2002, Railway applications, Current collection systems. Validation of simulation of the dynamic interaction between pantograph and overhead contact line, European Standard, (2002).
- [21] K.L.JONSON “Contact mechanics” Emeritus Professor of Engineering, University of Cambridge 2003.
- [22] Union Internationale des Chemins de fer. Code UIC 505-1.Union Internationale des Chemins de fer, 1997.

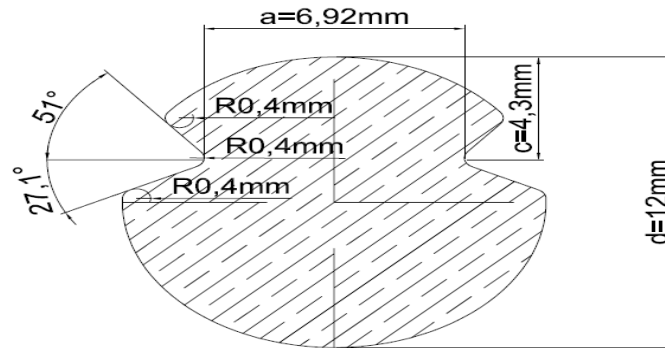
- [23] T. Kobayasi, Y. Jujihasi, T. Tsuburaya, J. ihi Satoh, Y. Oura, and A. Fujii, Current collecting performance of overhead contact line pantograph system at 425 km/h," *Electrical Engineering in Japan*, vol. E83-B, no. 3, pp. 609-615, May 1997.
- [24] L.M. Cléon, A. Bobillot, J.P. Mentel, E. Aziz: "OSCAR©: La caténaire en 3D". In *Revue Générale des Chemins de Fer*, Volume no.155, November 2006.
- [25] Intercity express programme: Trains technical specification document No.IEP-TEC-REQ-35; Issue 05
- [26] Surajit Midy "Conducted and Radiated Electromagnetic Interference in Modern Electrified Railways with Emphasis on Pantograph Arcing" June 2009
- [27] 9.4. Thomas, H. R., and Hoersche4w, V. A., Stress Due to the Pressure of One Elastic Solid upon Another, *University of Illinois Engineering Experimental Station Bulletin*, 212, 1930.
- [28] Thomas, H. R., and Hoersch, V. A., Stress Due to the Pressure of One Elastic Solid upon Another, *University of Illinois Engineering Experimental Station Bulletin*, 212, 1930.
- [29] K. Dang Van and H. Maitournam, "Fatigue Polycyclique des Structures", support de coursécole polytechnique, December 2008.
- [30] K. Dang Van and I. Papadopoulos, Eds., "High-Cycle Metal Fatigue in the Context of Mechanical Design", *CISM Courses and Lectures*, No.392, Springer-Verglas, 1999.
- [31] J. S. Kim, and B. D. Choi, "A study on Dynamic Characteristics of a Catenary System" *KSNVE*, 1999, Vol. 9, No. 2, 317~323.
- [32] W. M. Kim, J. T. Kim, J. S. Kim, and J. W. Lee, A numerical study on dynamic characteristics of a catenary, *KSME International Journal*, 2003, Vol. 17, 860~869
- [33] Azevedo CRF, Sinatora A. Failure copper contact strip. *Eng Fail Anal* 2004; 11:829–41.
- [34] Ning Zhou, Weihua Zhang. Dynamical performance simulation of the pantograph–catenary coupled system based on direct integration method. *China Acad Rail Sci* 2008; 29(6):71–6.

[35] Raymond L. Browell, "Predicting fatigue failure with Ansys work bench" 2006 international Ansys conference, may 2-4, 2006

[36] www.railwaypro.com

APPENDIX

A Contact Area cross section



B Application of Calculus variation

$$[m^{(e)}] \begin{Bmatrix} \ddot{v}_1 \\ \ddot{\theta}_1 \\ \ddot{v}_2 \\ \ddot{\theta}_2 \end{Bmatrix} + [k^e] \begin{Bmatrix} v_1 \\ \theta_1 \\ v_2 \\ \theta_2 \end{Bmatrix} = - \int_0^L [N]^T q(x, t) dx + \begin{Bmatrix} -V_1(t) \\ -M_1(t) \\ V_2(t) \\ M_2(t) \end{Bmatrix}$$

$$[m^e] = \rho A \int_0^L [N]^T [N] dx$$

Substitution for the interpolation functions and performing the required integrations gives the mass matrix as

$$[m^{(e)}] = \rho AL/420 \begin{bmatrix} 156 & 22L & 54 & -13L \\ 22L & 4L^2 & 13L & -3L^2 \\ 54 & 13L & 156 & -22L \\ -13L & -3L^2 & -22L & 4L^2 \end{bmatrix}$$

$$v_1 \quad \theta_1 \quad v_2 \quad \theta_2$$

$$K_e = \frac{EI}{L^3} \begin{bmatrix} 12 & 6L & -12 & 6L \\ 6L & 4L^2 & -6L & 2L^2 \\ -12 & -6L & 12 & -6L \\ 6L & 2L^2 & -6L & 4L^2 \end{bmatrix}$$

Eigen value equation $[K - \omega^2 M]\phi = 0$

C Contact Mechanics

$$z_1 = A_1x^2 + B_1y^2 + c_1xy$$

$$z_2 = A_2x^2 + B_2y^2 + C_2xy$$

$$A = \frac{1}{4} \left(\frac{1}{R_1} + \frac{1}{R_2} + \frac{1}{R_1^l} + \frac{1}{R_2^l} \right) - \frac{1}{4} \left\{ \left[\left(\frac{1}{R_1} - \frac{1}{R_1^l} \right) + \left(\frac{1}{R_2} - \frac{1}{R_2^l} \right) \right]^2 - \left[4 \left(\frac{1}{R_1} - \frac{1}{R_1^l} \right) \left(\frac{1}{R_2} - \frac{1}{R_2^l} \right) \sin^2 \theta \right] \right\}^{1/2}$$

$$B = \frac{1}{4} \left(\frac{1}{R_1} + \frac{1}{R_2} + \frac{1}{R_1^l} + \frac{1}{R_2^l} \right) + \frac{1}{4} \left\{ \left[\left(\frac{1}{R_1} - \frac{1}{R_1^l} \right) + \left(\frac{1}{R_2} - \frac{1}{R_2^l} \right) \right]^2 - \left[4 \left(\frac{1}{R_1} - \frac{1}{R_1^l} \right) \left(\frac{1}{R_2} - \frac{1}{R_2^l} \right) \sin^2 \theta \right] \right\}^{1/2}$$

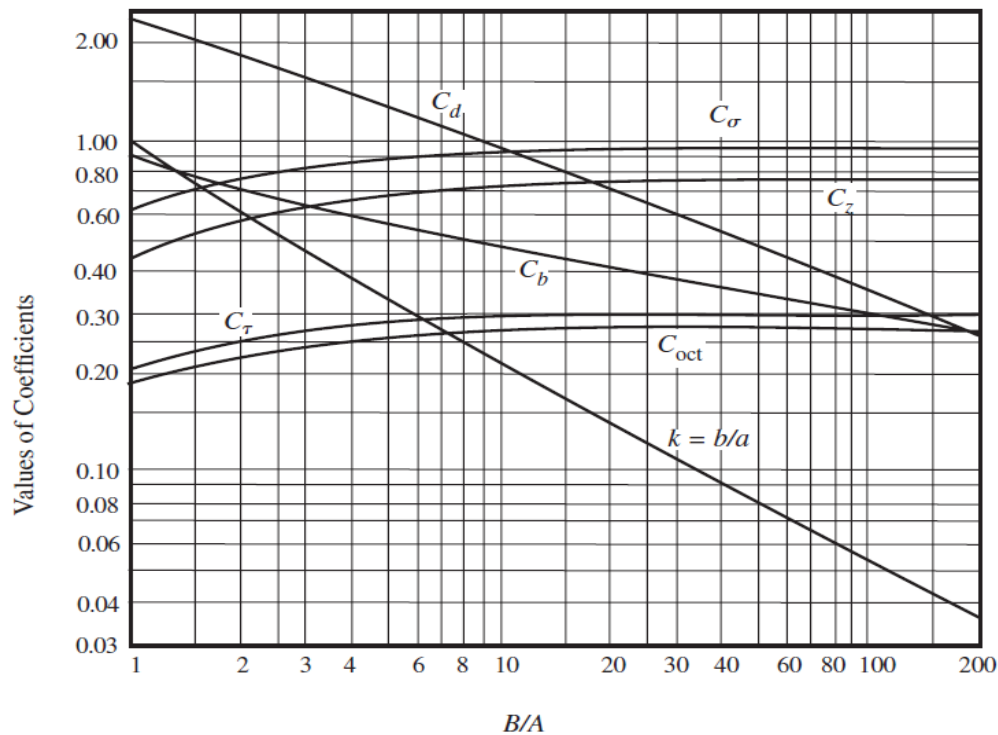
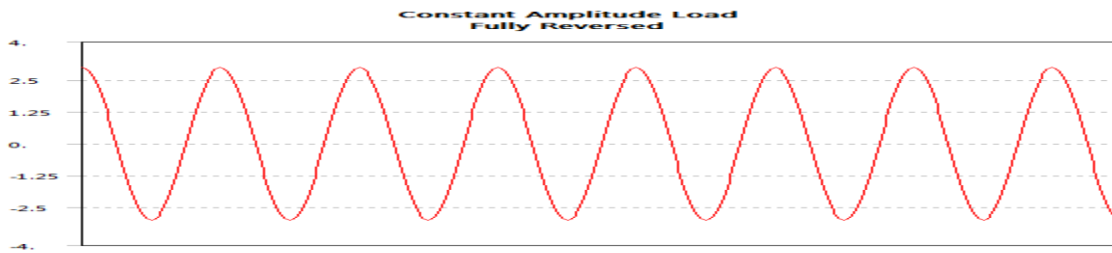


Figure of coefficients for contact

D Input data to Ansys workbench

Model 2 > Flexible Dynamic > Solution > Fatigue Tool



Modeling of contact wire-pantograph

Model 2 > Flexible Dynamic > Solution > Fatigue Tool

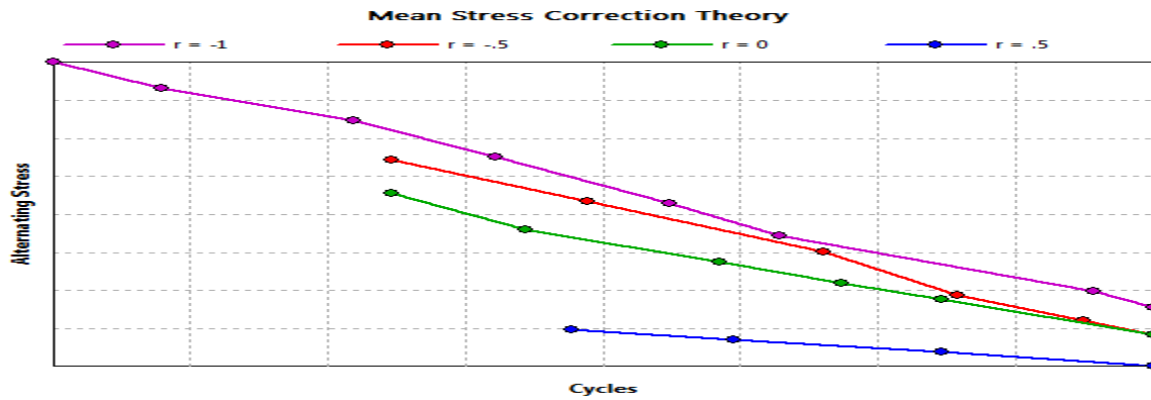


Figure 31: Mean stress correction

- Since the catenary wire is subjected to the cyclic load and it is considered (fully reversed) $r = -1$.

ADDIS ABEBA UNIVERSITY
ADDIS ABEBA INSTITUTE OF TECHNOLOGY
SCHOOL OF MECHANICAL AND INDUSTRIAL ENGINEERING

I, the undersigned, declare that this thesis with topic Developing pantograph-catenary contact and Predicting the fatigue life of the contact wire of rail ways is my original work and has not been presented for any masters program (degree) in any university and all the sources of materials used for the thesis have been duly acknowledged.

Andinet Zereabruk

Signature

Date

Name

.....

.....